TOPOLOGY OPTIMIZATION OF AN AIRCRAFT STRUCTURAL PART FOR ADDITIVE MANUFACTURING

MUSTAFA ÖZKARA

JUNE 2023

ÇANKAYA UNIVERSITY

GRADUATE SCHOOL OF NATURAL AND APPLIED SCIENCES

DEPARTMENT OF MECHANICAL ENGINEERING

M.Sc. Thesis in

MECHANICAL ENGINEERING

TOPOLOGY OPTIMIZATION OF AN AIRCRAFT STRUCTURAL PART FOR ADDITIVE MANUFACTURING

MUSTAFA ÖZKARA

JUNE 2023

ABSTRACT

TOPOLOGY OPTIMIZATION OF AN AIRCRAFT STRUCTURAL PART FOR ADDITIVE MANUFACTURING

ÖZKARA, Mustafa
M.Sc. in Mechanical Engineering

Supervisor: Assoc. Prof. Dr. Samet AKAR
June 2023, 78 Pages

Topology optimization is a powerful tool for creating high-performance parts that meet specific functional requirements while minimizing material usage and manufacturing costs. It typically involves creating a digital model of the part, defining the functional requirements and constraints, and using software algorithms to generate a range of possible designs. Although this tool has been used for many years, there have always been many problems in the manufacture of optimized parts. As technology develops, there have been significant developments in various manufacturing techniques to be able to implement optimized parts for industries. One of the most important techniques is additive manufacturing (AM). The combination of topology optimization and AM has brought several advantages to eliminating the manufacturing difficulties of the parts that are topologically optimized, especially in the aerospace industry. With these developments, the optimized design can be produced using AM and the final part can have a geometry designed according to its intended use. This thesis provides an overall study of optimization advantages by making comparisons using parts that are designed and analyzed with traditional and additive manufacturing techniques per different AM materials.

Keywords: Additive manufacturing, Additive manufacturing materials, Topology optimization, Aircraft structures, Ti-6Al-4V, AlSi10Mg

ÖZET

BİR UÇAK YAPISAL PARÇASININ KATMANLI İMALAT İÇİN TOPOLOJİ OPTİMİZASYONU

ÖZKARA, Mustafa
Makine Mühendisliği Yüksek Lisans

Danışman: Doç. Dr. Samet AKAR
Haziran 2023, 78 sayfa

Topoloji optimizasyonu, malzeme kullanımını ve üretim maliyetlerini en aza indirirken belirli işlevsel gereksinimleri karşılayan yüksek performanslı parçalar oluşturmak için güçlü bir araçtır. Tipik olarak, parçanın dijital bir modelini oluşturmayı, işlevsel gereksinimleri ve kısıtlamaları tanımlamayı ve bir dizi olası tasarım oluşturmak için yazılım algoritmalarını kullanmayı içerir. Bu araç uzun yıllardır kullanılmasına rağmen, optimize edilmiş parçaların imalatında her zaman birçok sorun olmuştur. Teknoloji geliştikçe, endüstriler için optimize edilmiş parçaları uygulayabilmek için çeşitli üretim tekniklerinde önemli gelişmeler olmuştur. En önemli tekniklerden biri eklemeli imalattır (AM). Topoloji optimizasyonu ve AM kombinasyonu, özellikle havacılık endüstrisinde topolojik olarak optimize edilmiş parçaların üretim zorluklarını ortadan kaldırmak için çeşitli avantajlar sağlamıştır. Bu geliştirmeler ile optimize edilmiş tasarım AM kullanılarak üretilebilir ve son parça kullanım amacına göre tasarlanmış bir geometriye sahip olabilir. Bu tez, farklı AM malzemelerine uygun olarak geleneksel ve eklemeli üretim teknikleriyle tasarlanan ve analiz edilen parçaları kullanarak karşılaştırmalar yaparak optimizasyon avantajlarının genel bir çalışmasını sağlar.

Anahtar Kelimeler: Eklemeli imalat, Eklemeli imalat malzemeleri, Topoloji optimizasyonu, Uçak yapıları, Ti-6Al-4V, AlSi10Mg

ACKNOWLEDGEMENT

I would like to express my sincere gratitude to my advisor Assoc. Prof. Dr. Samet AKAR for his invaluable guidance and support throughout my master's program. His expertise and encouragement helped me to complete this research and write this thesis. I am also thankful for his understanding of the difficulties I have experienced as I was trying to manage my thesis program and my business together.

I sincerely thank my family for their support during my master's thesis and their understanding during my stressful times. Without their loving support and patience, I would not have been able to complete this challenging process. Knowing that they are always by my side has strengthened me and helped me move forward.

Words cannot express my gratitude to my invaluable source of strength and encouragement Öykü Kurt, for her endless understanding of my master's thesis and for enabling me to achieve success through the work we have done together. Without her love and support, I would not have made it this far on this journey.

TABLE OF CONTENTS

LIST OF TABLES

LIST OF FIGURES

LIST OF ABBREVIATIONS

ABBREVIATIONS

FEA	: Finite Element Analysis
AM	: Additive Manufacturing
3D Printing	: 3-Dimensional Printing
EOP	: Edge of Part
UV Laser	: Ultraviolet Laser
LEAP	: Leading Edge Aviation Propulsion
PBF	: Powder Bed Fusion
FDM	: Fused Deposition Modelling
SLS	: Selective Laser Sintering
EBM	: Electron Beam Melting
UTS	: Ultimate Tensile Strength
YS	: Yield Strength
E	: Young's Modulus
CoG	: Center of Gravity
MMPDS	: Metallic Materials Properties Development and Standardization
Al	: Aluminum
Ti	: Titanium
SF	: Safety Factor
SLM	: Selective Laser Melting
UD	: Unidirectional

CHAPTER I
INTRODUCTION

With the improvements in software technology, studies in many areas have evolved into searches for optimizing outputs. Optimization aims to find the best solution among all possible alternatives, given a set of constraints and a defined objective function. It can be involved in many research and business areas such as engineering, finance, industry etc. It generally aims to reduce cost, production time or any constraint considering given inputs and outputs to be achieved.

With the developments in technology, many methods have become available thanks to computers and software. As in many areas, it has been always a trending topic in the engineering field [1]. In engineering optimization weight, production time and cost can be limiting factors for optimization studies. For structural optimization, it refers to a highly advanced approach to designing structures that involves achieving the most effective configuration through the distribution of materials that meets specific load conditions, constraints, and performance criteria [2].

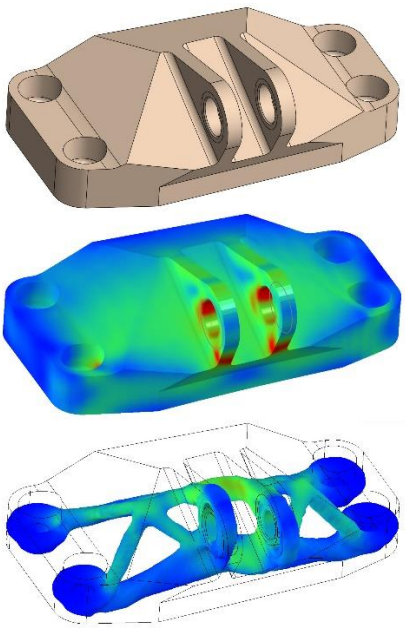

Figure 1: Topology Optimization Example of a Bracket [3]

As Figure 1 shows, the initial mass of the bracket is higher than the condition, which applied topology optimization. By using software, calculations are made to remove unnecessary material in the specified domain.

It should also be considered that manufacturing limitations may affect the final design. If it cannot be produced by any manufacturing method, the part becomes useless for any engineering field, even topology optimization presents the ideal geometry.

Additive manufacturing, also known as 3D printing, is a process of creating three-dimensional objects by adding layers of material one by one. This contrasts with traditional manufacturing methods, which typically involve subtractive processes (such as cutting or drilling) or molding and casting. It enables engineers to overcome the limitations of traditional manufacturing methods when creating topology-optimized structures, thereby allowing them to focus primarily on designing lightweight and high-performance structures [2].

The designs with lattice structures that can be easily produced through additive manufacturing technologies are the best examples of this situation in the field of mechanical engineering. The motivation behind for implementation of lattice structures in designs is reducing weight and enhancing multifunctional features. Topology optimization, which is one of the methods used to produce lattice structures, has been noted as an effective tool to obtain optimal forms [4].

1.1 OBJECTIVE

Topology optimization has proven to be a useful technique in achieving designs that are lightweight and high-performance, particularly in the fields of aeronautics and aerospace engineering [5]. In this study, an aircraft part that is currently used in service is optimized by considering manufacturing and installation constraints by using ANSYS.

The objective of this study is to demonstrate that additive manufacturing expands the possibilities of creating lighter designs without sacrificing any functionality. The resulting design will be compared to a conventionally sized design.

1.2 ORGANIZATION OF THESIS

There are five chapters in this thesis. In Chapter 1, an introduction is given to provide brief information about the scope of the thesis. Chapter 2 covers the literature

survey and studies about topology optimization and current technologies in additive manufacturing. Chapter 3 includes all the analyses and studies of an aircraft structural part which is the main purpose of this thesis. In Chapter 4, the effects of production direction in AM on optimization analyses related to anisotropy are researched. Chapter 5 provides all the study results and the discussion about these results.

CHAPTER II
BACKGROUND AND LITERATURE SURVEY

From the beginning of structural design, it is always desired to have lightweight and stiff parts. With this motivation, many researchers have studied optimization over decades [6]. Although optimization has been developed by computer technology, manufacturing limitations prevent obtaining the maximum benefits of optimized parts [7]. Thanks to additive manufacturing, production problems have been solved nowadays, but still, there are many problems that should be considered [2].

2.1 TOPOLOGY OPTIMIZATION

Structural optimization refers to a process of designing and analyzing a structure to achieve the best possible performance under specified conditions, subject to constraints such as size, weight, strength, and cost. The goal of structural optimization is to find the optimal shape, size, and configuration of a structure to maximize its performance while minimizing the material and manufacturing costs.

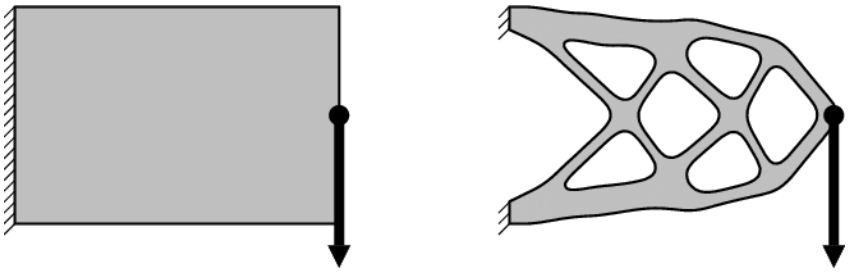

Figure 2: 2D Structural Optimization Example [8]

There are several types of structural optimization, including topology optimization, shape optimization and size optimization. Size optimization refers to a process of determining the optimal cross-section dimensions of each element in a structure to vary its measurements to achieve the ideal form. Shape optimization involves improving the outer features of the structure, leaving its connections as are. Topology optimization explains how the elements that make up the structure can be connected in the best way [9]. Among these optimization types, topology optimization

is the most comprehensive method as it provides new design ideas for engineers and designers without the need for preliminary design [10].

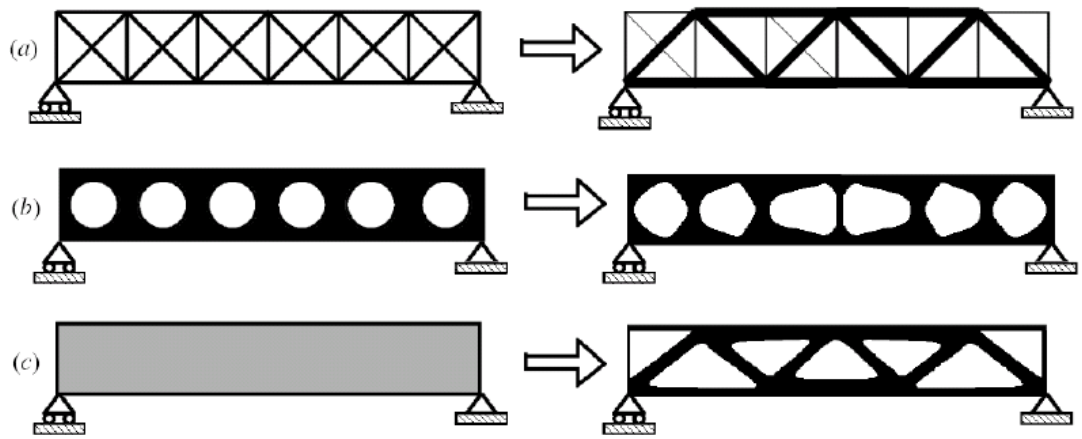

Figure 3: Examples of Sizing Optimization(a), Shape Optimization(b) and Topology Optimization(c) [11]

2.1.1 Topology Optimization Procedure

The first step is the structural problem definition step where a designer or engineer will define the design domain and its boundary conditions, loads and constraints. The user generally shares this information through a user graphic interface of an analysis program. The design domain is the maximum usable volume of the part that will be optimized. Next, the design area created by the user is transformed into a model made up of smaller parts, known as finite elements, to better understand the stresses and strains of each part. By carrying out analyses for the initial part with these inputs, displacements and stresses are found. Then, topology optimization eliminates material from regions that do not play a significant role in supporting the applied loads, as determined by the stress and displacement distribution. The design is improved using a chosen optimization approach, and the new structure is examined once again using advanced calculation methods for finite elements.

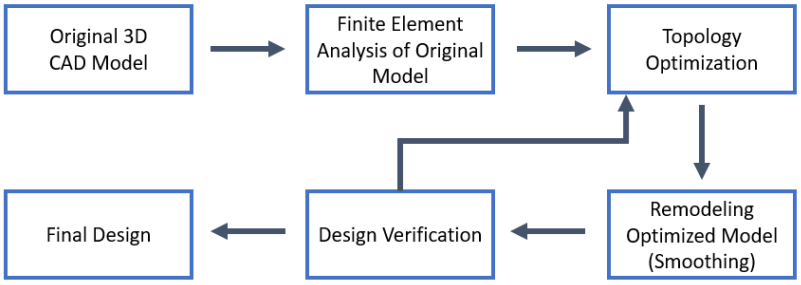

Figure 4: Topology Optimization Procedure

This back-and-forth process is repeated many times, sometimes even a hundred times, until the best possible design is found. Figure 4 and Figure 5 show optimization steps to better understand the whole process and the iteration sequence of the analyses.

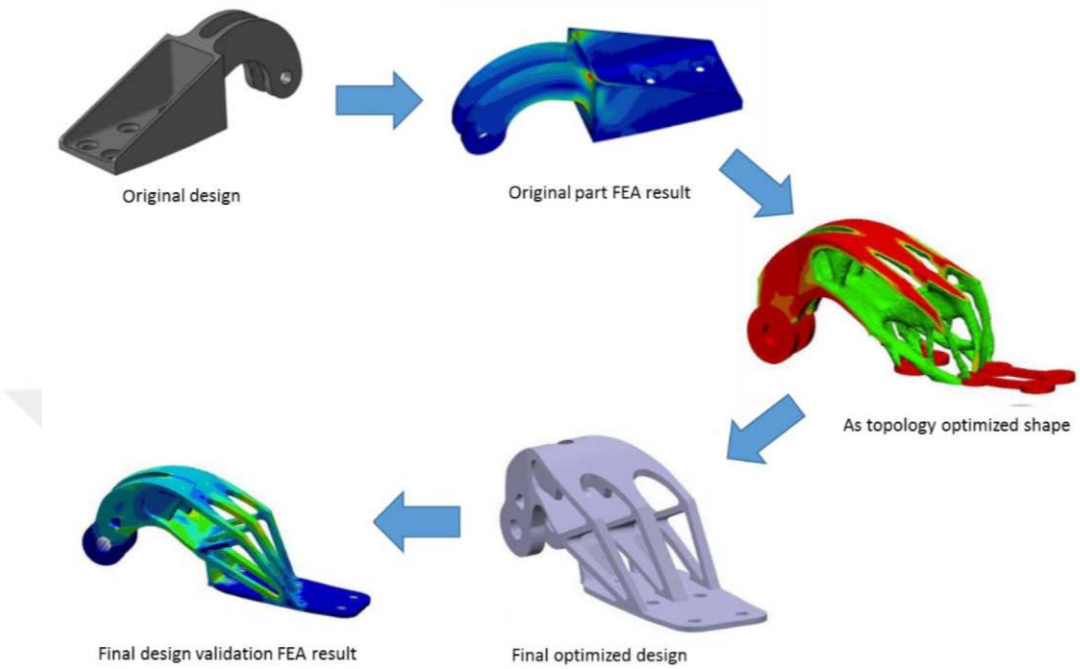

Figure 5: Topology Optimization Process [12]

2.1.2 Topology Optimization History and Methods

The beginning of the search for lightweight design solutions is the studies of A.G.M Michell [13] an Australian engineer [14]. Michell searched for the optimal material distribution by using truss structures that can carry only tension and compression loads. Finding the optimal layout of truss structures by determining the most efficient arrangement can be accepted as the first structural optimization concept in the literature and it has inspired further developments.

After Michell, many methods and research are worked in the last 100 years. In the year 1988, a seminal work of Bendsøe and Kikuchi [15] has become the beginning of the modern era of topology optimization. Their work expanded the applicability of topology optimization beyond trusses to continuum structures, which significantly broadened its scope in engineering and design.

Their approach to topology optimization was based on homogenization, which assumed that the structure was made up of non-homogeneous elements consisting of solid and void regions. They used an optimization process to obtain an optimal design

while considering the volume constraints. In their methods, areas with dense cells are defined as structural volumes, while areas with empty cells are considered unnecessary material [16]. Thomsen [17] discussed the use of the homogenization technique to maximize the integral stiffness of a structure made of one or two isotropic materials with high stiffness in 1992.

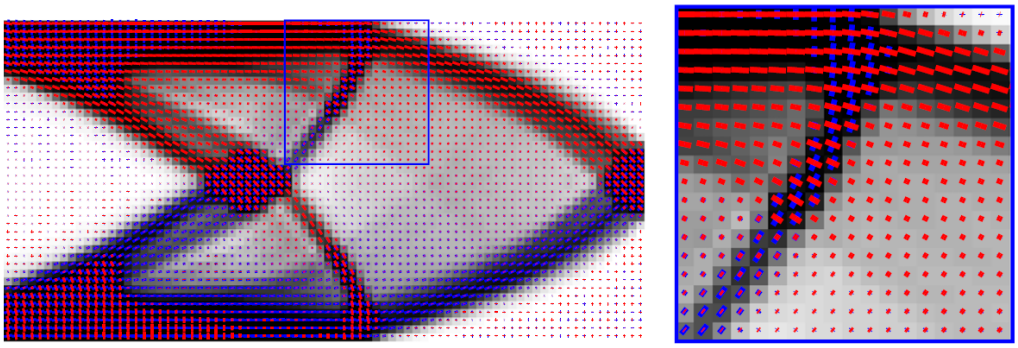

Figure 6: Homogenization-based Optimized Topology Example [18]

Since then, many different topology optimization techniques have been developed, including density-based method, evolutionary structural optimization (ESO), and level set method (LSM) [2].

2.1.2.1 Solid Isotropic Material with Penalization (SIMP)

One of the most popular approaches to topology optimization, the density-based approach, was set by the key research of Bendsøe [19] and Rozvany and Zhou [20]. The density-based method transforms a 0-1 discrete optimization problem into a continuous optimization problem to enable the relaxation of the binary design form. The homogenization method was initially used to map a specified microstructure controlled by density variables to effective properties, but it is difficult to implement due to mathematical complexity [2].

After all, an alternative approach is proposed called Solid Isotropic Material with Penalization (SIMP). The SIMP method is a popular topology optimization technique that penalizes the element elastic modulus exponentially based on density variables compared with homogenization [2]. It has a compact form and is widely embedded in commercial software to solve engineering problems.

The distribution of material is achieved by adjusting the densities of elements within the mesh as mentioned before. However, in traditional methods, the distribution is made by assigning the design domain, ρ, a binary value:

- $\rho_{(e)}$ = 1 where material is used
- $\rho_{(e)}$ = 0 where material is not used

With the introduction of a relative density function, the density can vary between a minimum value ρ_{min} and 1 so that there can be elements with intermediate densities. The minimum allowable relative density value for empty elements greater than zero is denoted as ρ_{min}. This specific density value is crucial to maintaining the numerical stability of the finite element analysis.

The penalty factor, denoted as 'p', reduces the impact of elements with intermediate densities (gray elements) on the overall stiffness, which is the penalization portion of SIMP. This factor is used to guide the optimization solution towards elements that are either fully solid black ($\rho_{(e)}$ = 1) or completely void white ($\rho_{(e)}$ =ρ_{min}). The formulation is as follows:

$$\begin{gathered} Minimize\ Compliance:\ c(\rho) = U^T K U = \sum_{e=1}^{N} (\rho_e)^p u_e^T k_e u_e \\ Subject\ to: \frac{V_{(\rho)}}{V_0} = f \\ KU = F; \\ 0 < \rho_{min} \leq 1; \end{gathered} \tag{2.1}$$

Where c is the compliance, N is the number of elements, u_e is the elemental displacement vector, k_e is the elemental stiffness matrix, U is global displacement vector, K is global stiffness matrix. In addition, F is global force vector and V is the volume of the design.

2.1.2.2 Evolutionary Structural Optimization (ESO)

Evolutionary Structural Optimization (ESO) is a topology optimization method that is inspired by the evolutionary processes found in nature. Since it was proposed by Xie and Steven [21], it has become one of the most widely used topology optimization methods.

It starts with an initial design, often a fully solid structure, and iteratively removes material based on a performance measure until an optimal design is achieved. The concept behind this idea is simple and empirical. It involves the gradual removal of elements with the lowest stresses, as a means of allowing the structure to evolve towards an optimal state [22]. The ESO principle is based on the discrete design

variable method (also called the "hard kill" method), as opposed to the continuous design variable approach utilized in SIMP (known as the "soft kill" method). The hard kill parametrization in ESO involves the local addition or removal of high-conductivity material in a single step, while the soft kill method in SIMP increases or decreases it gradually and by small amounts [23].

ESO has several advantages, such as its simplicity, ease of implementation, and ability to handle various types of optimization problems. However, it also has some limitations. For instance, ESO may not be as effective for problems where adding material is necessary to achieve an optimal design. To solve these issues, researchers have developed the Bi-directional Evolutionary Structural Optimization (BESO) method [24, 25], which extends the ESO concept by including the addition of material during the optimization process.

2.1.2.3 Level Set Method (LSM)

The level set method is a boundary-based approach for topology optimization that represents the structure's boundary as the zero-level set of a higher-dimensional function, called the level set function [2]. It offers advantages such as smooth boundary representation, the ability to handle complex topologies, and ease of managing topological changes during topology optimization.

The LSM method was first used by Osher and Sethian [26] for modeling moving boundaries. After that, Haber and Bendsøe [27] used this level-set-based concept for Topology Optimization in 1998. Then, many researchers started to work on this new concept [28].

With its ability to handle complex topologies and represent smooth boundaries, it has become a popular choice for topology optimization problems that involve intricate designs or require a high level of detail.

2.2 ADDITIVE MANUFACTURING

Additive manufacturing (AM) or 3D printing is a method that enables the production of parts with complex geometries by adding the material layer by layer different from the traditional production methods, which remove material from bulk. Figure 7 shows a brief example of the comparison between traditional manufacturing and additive manufacturing.

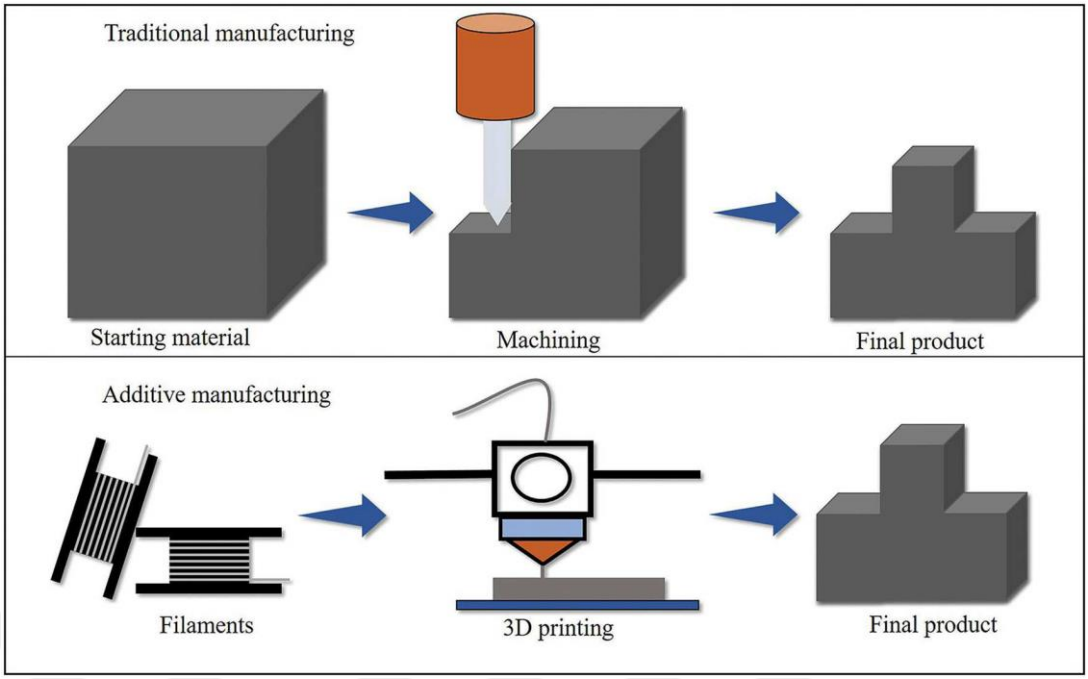

Figure 7: Comparison Between Traditional Manufacturing Technique and Additive Manufacturing [29]

Since its first steps in the 1980s, the technology has evolved significantly over the years with numerous innovations and advances leading to the development of various additive manufacturing processes [30].

The first product capable of 3D manufacturing is the Stereolithography Apparatus, developed and patented by Chuck Hull in 1984 [31]. After that, he co-founded 3D Systems, so the world's first 3D printing company has been established. With this invention, Stereolithography (SLA) became the first 3D manufacturing method.

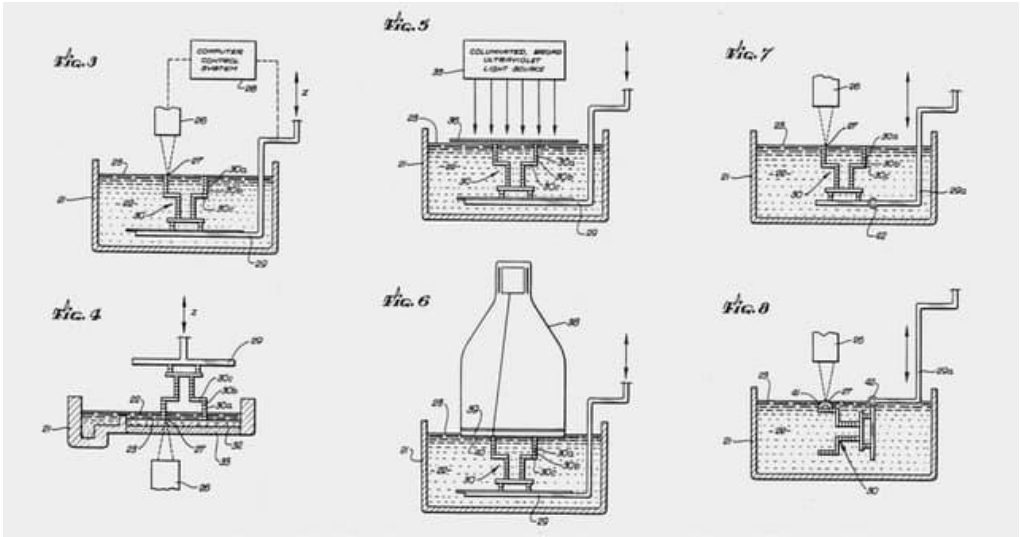

Figure 8: Stereolithography Apparatus Patent [31]

After Chuck Hull, the second biggest development of 3D manufacturing took place. In 1989, Scott Crump developed Fused Deposition Modeling (FDM), a process that extrudes thermoplastic material through a heated nozzle, depositing it layer by layer to form a 3D object. Crump patented the technology the same year [32]. With this patent, he and his wife, Lisa Crump, co-founded Stratasys Ltd. which later became one of the leading companies in the additive manufacturing industry.

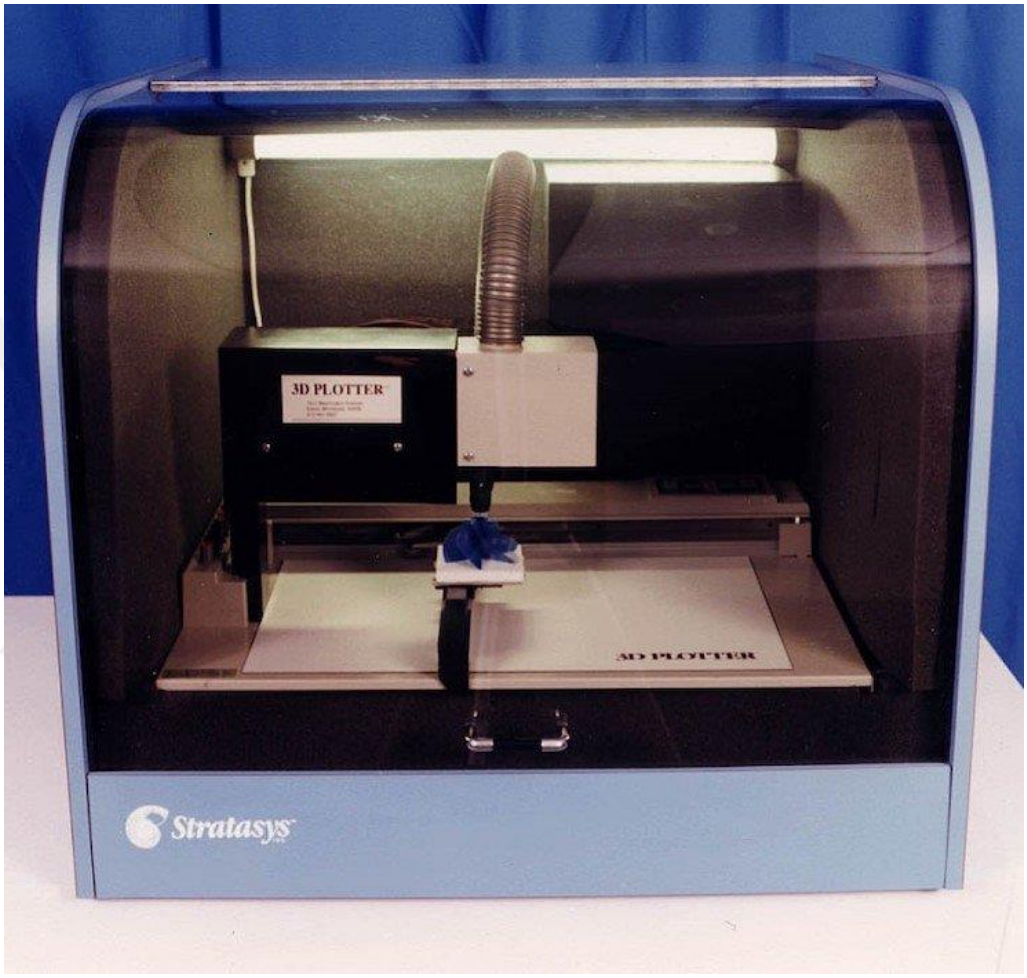

Figure 9: Stratasys' First Operating 3D Printer [33]

With these steps in 3D manufacturing, many researchers and companies focused on this new production technology. From construction to biomedical applications, it has been a trending topic because of its low cost and easy product renewability [34].

2.2.1 Additive Manufacturing Methods

Many methods have been developed since SLA was invented. As mentioned earlier, many companies work to apply the right method according to their field of application because each method has its strengths and weaknesses.

2.2.1.1 Stereolithography (SLA)

SLA uses a UV laser to selectively cure a liquid photopolymer resin, solidifying it layer by layer to create a 3D object. This method is known for its high resolution and smooth surface finish but may require support structures for overhanging parts.

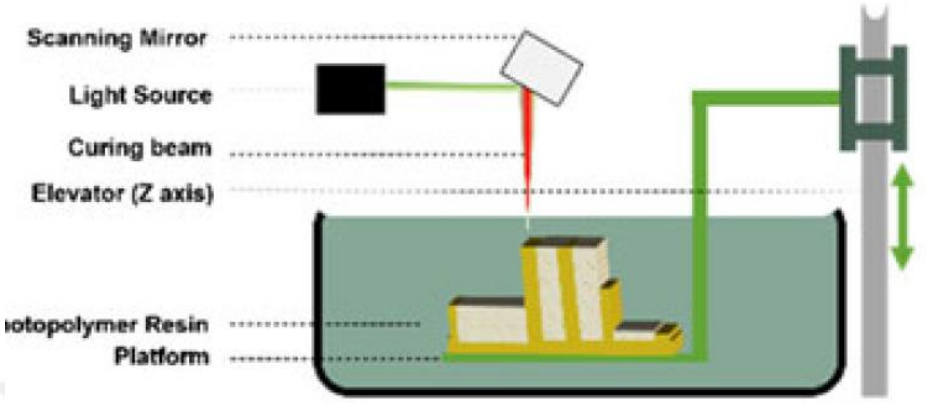

Figure 10: Illustration of SLA Method [35]

2.2.1.2 Fused Deposition Method (FDM)

FDM extrudes thermoplastic material through a heated nozzle, depositing it layer by layer to form a 3D object. This technique is widely used due to its affordability and versatility in materials, but it typically has a lower resolution and surface finish compared to other methods.

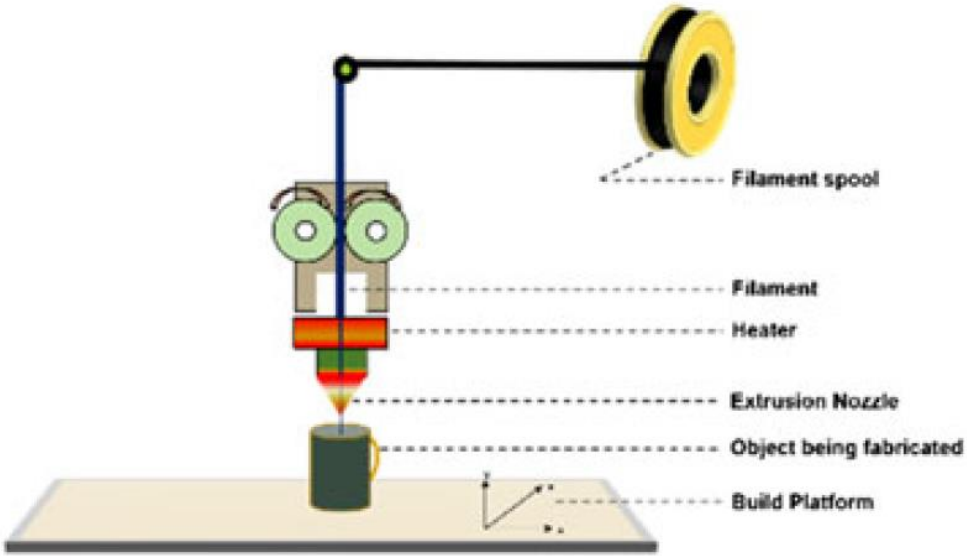

Figure 11: Illustration of FDM Method [35]

2.2.1.3 Selective Laser Sintering (SLS)

SLS uses a high-power laser to fuse powdered material (such as nylon, polystyrene, or metal) layer by layer, creating a solid 3D object. This method can

produce strong, durable parts without the need for support structures, but it often requires specialized equipment and post-processing.

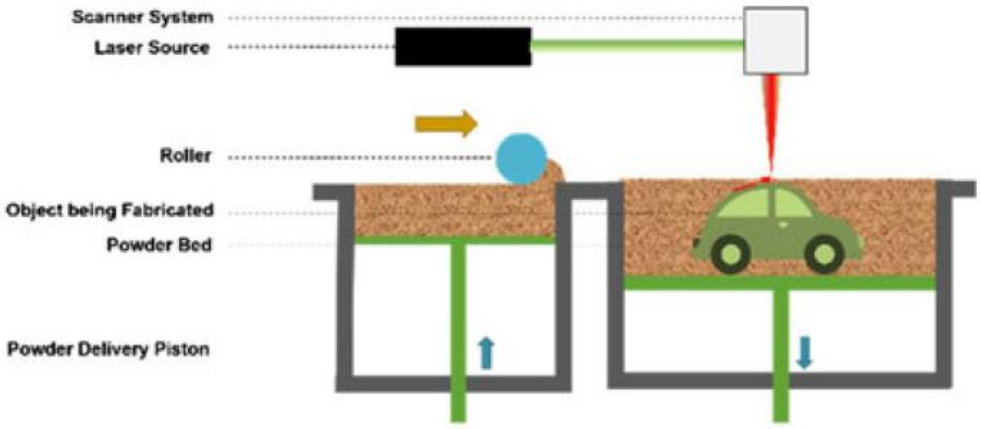

Figure 12: Illustration of SLS Method [35]

2.2.1.4 Binder Jetting

This technique involves depositing a liquid binder onto a powder bed and bonding the particles together to create a solid object. The process is suitable for various materials, including metals, ceramics, and sand. Binder jetting can produce parts quickly and at a lower cost, but they usually have lower strength and require post-processing.

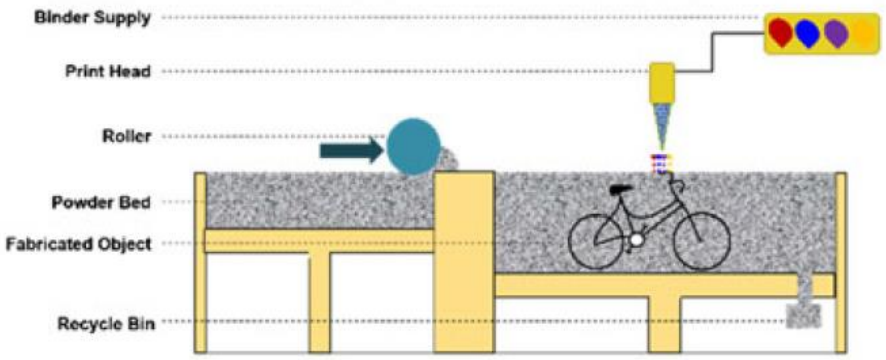

Figure 13: Illustration of Binder Jetting Method [35]

2.2.1.5 Electron Beam Melting (EBM)

Like SLS, EBM uses an electron beam to melt powdered metal materials in a vacuum chamber. EBM can produce complex, high-strength metal components, but the process is slower and more expensive than other methods. Due to its high strength properties, it can be used in the aerospace industry in the production of structural parts such as turbine blades and fuel nozzles, which must withstand extreme temperatures and stresses.

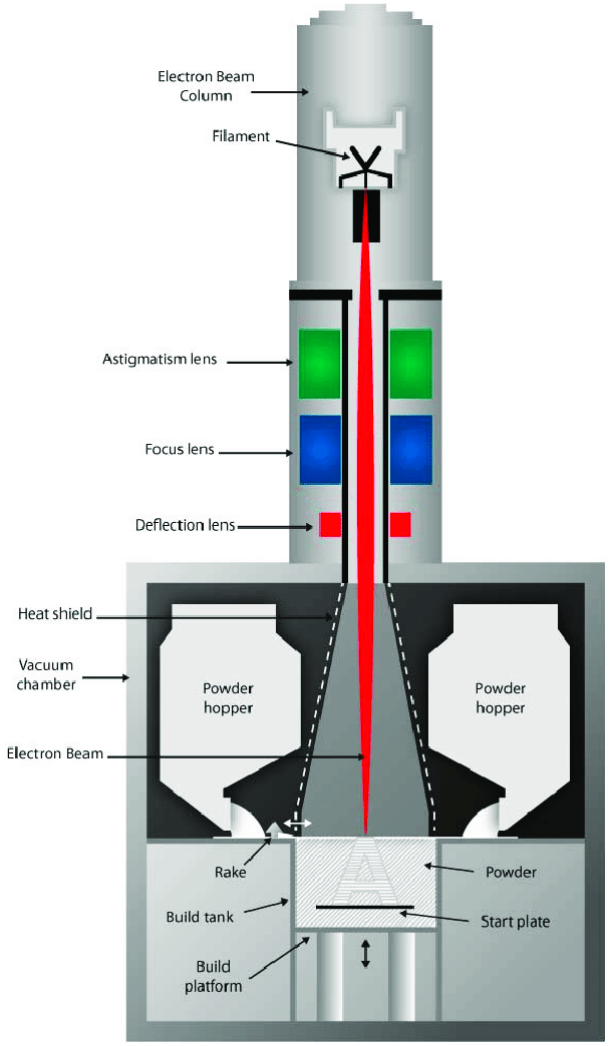

Figure 14: Illustration of EBM Method [36]

2.3 TOPOLOGY OPTIMIZATION FOR ADDITIVE MANUFACTURING

The increase in the possibility of using additive manufacturing has paved the way for the use of this new technology for topology optimization. The main problem of topology optimization is the manufacturability of the optimized parts because, in optimization, the main goal is reducing the material in volumes that are not needed. Even if the mass of the final design is reduced, there might be volumes with complex geometries which cannot be manufactured by using traditional manufacturing methods. Nevertheless, it is possible to manufacture these complex parts with additive manufacturing. AM allows for greater design freedom and the production of complex geometries that were previously unattainable. Combining AM with topology optimization opens new possibilities for lightweight and high-performance components.

As in many areas, aerospace companies are also trying to adapt to this new opportunity. Since mass is the main determinant for any aircraft, it is extremely advantageous to use topology optimization for structural parts. An example of using additive manufacturing is the fuel nozzle tip for CFM LEAP engines of GE Aviation. The company shipped its 100,000th 3D-printed nozzle tip in 2021 [37]. So, it showed that mass production can also be possible with additive manufacturing.

Figure 15: 3D Printed Nozzle Tip [37]

2.3.1 Manufacturing Constraints for Optimized Parts

Although it seems like there will be no manufacturing limitations, additive manufacturing has its own constraints such as minimum length, connectivity, overhang, and anisotropy. Combining these constraints with topology optimization will provide realistic and reliable results for the design engineers to achieve the maximum efficiency of additive manufacturing which is the most accepted and currently studied method among new manufacturing techniques [5].

2.3.1.1 Minimum Length

AM technologies have limitations on the minimum feature size that can be accurately printed, based on factors such as the resolution of the printer and the material being used. Designs with features smaller than the minimum allowable size may result in incomplete or inaccurate parts.

Directly additively manufacturing topology-optimized structures can be challenging so it is essential to apply length scale restrictions during topology optimization to prevent the creation of non-manufacturable geometric features [2].

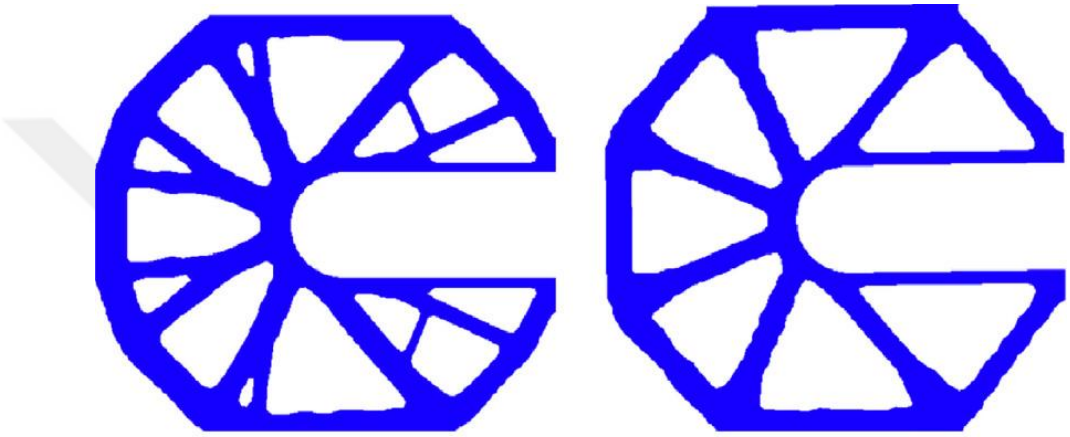

Figure 16: Topology Optimization Example without(left) and with(right) Minimum Length Constraint [2]

2.3.1.2 Connectivity

One of the most critical constraints in Additive Manufacturing is the removal of unused powder in Powder Bed Fusion [38]. In this method, the part is produced by melting or fusing the metal powders regarding the area of the layer. After manufacturing is done, the final design must not contain any enclosed voids, as this is crucial for powder-based additive manufacturing methods. If optimized structures possess enclosed voids, they will trap unmelted powder, leading to increased weight [39]. To create lightweight designs and enable the recycling of unmelted powder, it is essential to eliminate any unmelted powder trapped within enclosed voids.

Recently, Zhao et al. [40] introduced a successful method for managing structural connectivity in topology optimization. This technique allows for a harmonious balance between structural performance and the impact of controlling structural complexity.

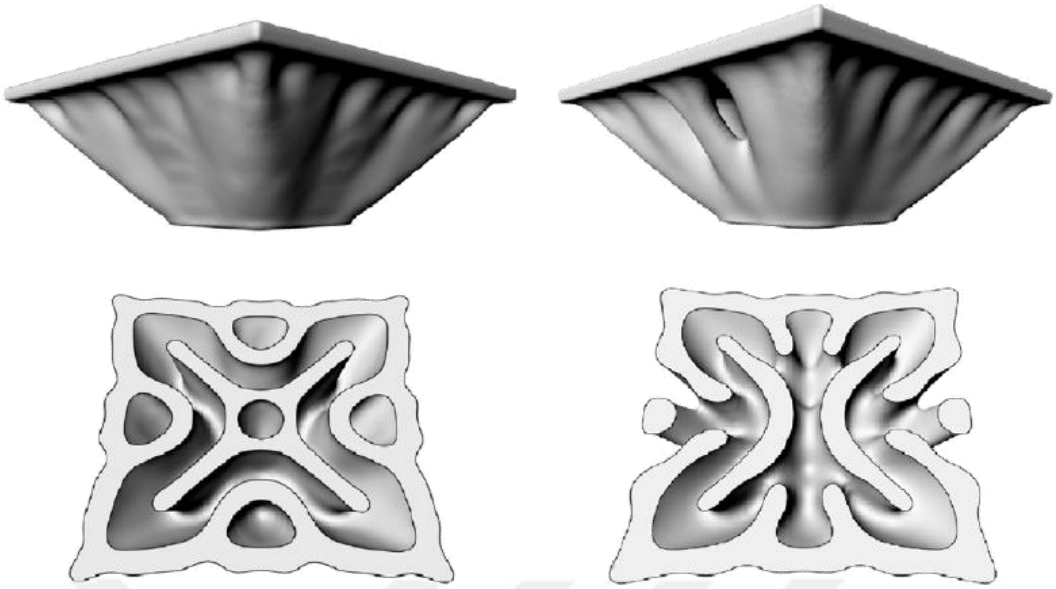

Figure 17: Example of Optimization Without Connectivity Constraint(left) and With Connectivity Constraint(right) [2]

2.3.1.3 Overhang

For many AM methods, the feature angle has significant importance. When a specific angle is reached (typically 45 degrees relative to the build platform) or a feature is entirely overhanging, these areas lack support, which often fails [7]. To solve problems associated with these overhanging elements, temporary support structures are created to facilitate geometries that exceed the angle limit. However, these supports increase both time and material consumption during the manufacturing process and adversely impact the final part's surface quality, as they must be subsequently removed during post-processing [41].

To overcome this issue, it is better to implement an overhang constraint to topology optimization so that any support structure is not needed.

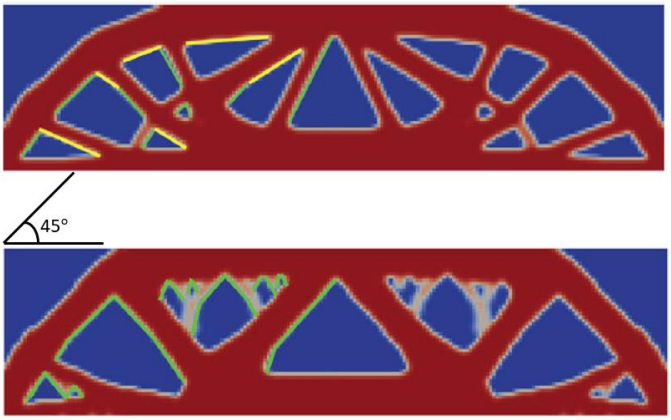

Figure 18: Comparison of Topology Optimization Before and After Overhang Constraint [2]

2.3.1.4 Anisotropy

Anisotropy is an important challenge in Additive Manufacturing. Due to the layer-by-layer manufacturing process, the material's microstructure within each layer differs from that at the interfaces between layers. This anisotropic behavior leads to varying mechanical properties in 3D printed components when subjected to tension or compression, as opposed to their performance in the horizontal direction [34].

During the process, the layers are typically bonded together using techniques like melting, sintering, or curing. As the layers are stacked and bonded, the mechanical properties of the printed object can differ along the build direction compared to the plane of the layers.

The method in which anisotropy is observed the highest is FDM and 50% difference may occur in the parts [42]. This ratio may decrease to 10% for SLS and to approximately 1% for SLA method [42].

Yiğitbaşı S. studied the mechanical properties of Ti64 samples manufactured in the x-y-z direction [43]. The samples are manufactured with EBM method and all samples are machined after production for cleaning the support structures and improving the surface roughness to be able to obtain the same conditions for different samples. Figure 19 shows the building directions of the specimens.

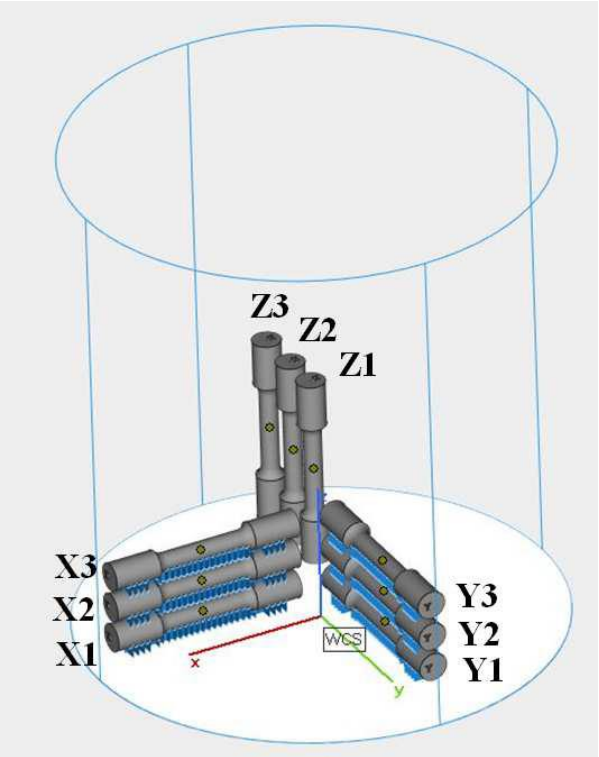

Figure 19: Building Directions [43]

All the samples have been exposed to tensile force with a tensile test setup. The results show that there is a difference between the directions and strengths.

Table 1: Mechanical Properties of the Samples

	X Samples	**Y Samples**	**Z Samples**
Ultimate Tensile Strength [MPa]	967 ± 29	988 ± 13	1023 ± 21
Yield Strength [MPa]	852 ± 16	895 ± 14	940 ± 23
Young's Modulus [GPa]	155 ± 17	136 ± 17	158 ± 22

Z specimens that were built parallel to the applied force, have better results on UTS, YS and E than X and Y specimens that were built perpendicular to the applied load. Given that, both X and Y specimens are manufactured in the same orientation with tensile test applied load, variations in scanning strategies could account for the differences between them [43].

Other studies in anisotropy show that there are differences in strength values according to building orientation [44, 45, 46, 47, 48]. However, topology optimization has predominantly used idealized isotropic material models, which neglect the influence of material anisotropy on both the design and performance of the structure [2].

CHAPTER III
IMPLEMENTATION AND OPTIMIZATION OF AN AIRCRAFT PART

In this thesis, a currently used aircraft part will be re-designed and optimized by considering additive manufacturing constraints. The main purpose of the study is to show how successful the combination of topology optimization and additive manufacturing is and can be used to create effective parts in the future. As mentioned before, there are many challenges and limitations in this technology but by considering appropriate constraints, successful studies can be achieved.

3.1 DEFINITION AND AIM OF THE PART

An average military aircraft has thousands of parts. Most of this number consists of structural parts. While the main task of these parts is to carry the flight loads, they are also responsible for carrying the avionics systems components which are the electronic systems of the aircraft.

Structural parts can be mainly divided into two categories according to their requirements:

- Structural Airframe Parts
- System Installation Parts

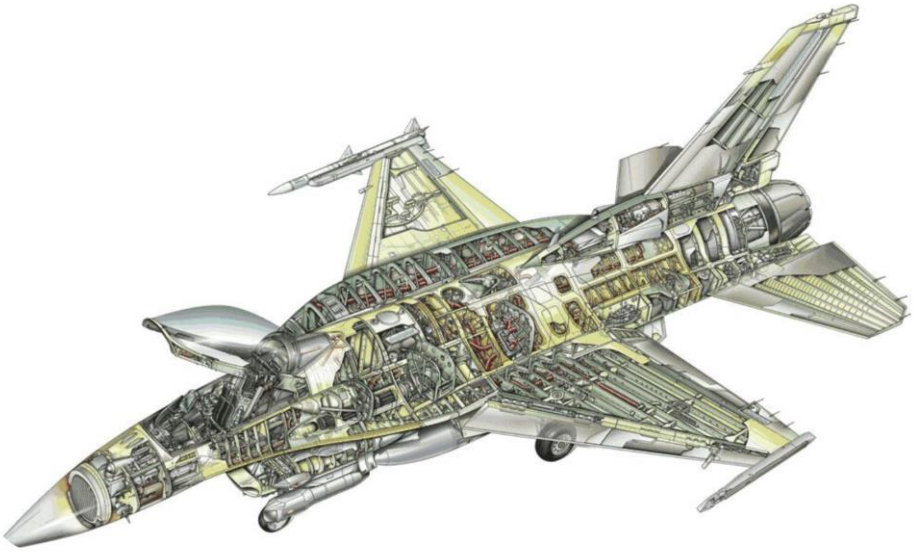

Figure 20: Sectioned View of F-16

Structural airframe parts are supposed to carry all aerodynamic loads, inertia loads, and loads that can be occurred during extreme maneuvers. In general, they provide structural integrity for the aircraft. They also provide a connection interface for the installation parts. Examples of this category can be given as frames, spars, longerons, wing-body fittings, etc.

On the other hand, system installation parts are responsible for carrying inertia and abuse loads of the avionic components and other required components for many different systems and sub-systems.

The part that will be studied is a system installation part and the only load which will be considered is the inertia loads of a component connected to it by removal fasteners. The part should carry a component that has approximately 12 kg mass.

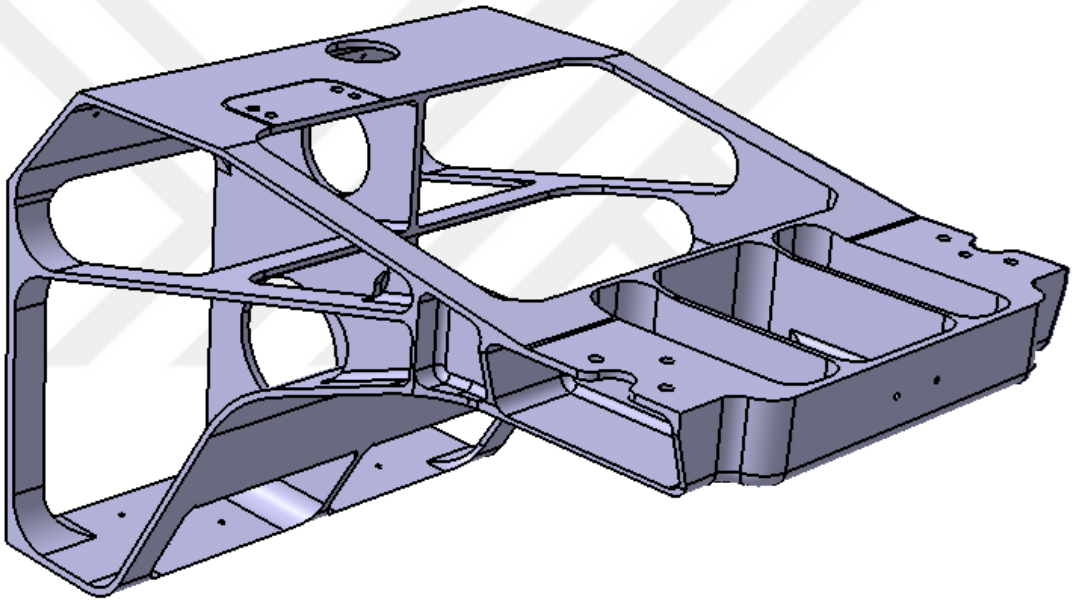

Figure 21: A Picture of the Currently Used Part

Figure 21 shows the part which is currently in service. The material is AL 7050 and it is manufactured by using traditional machining techniques and also it has a mass of 1.712 kg. The motivation for choosing this installation part is to provide a comparative study between the initial optimized part for traditional manufacturing methods and a new design that will be optimized according to additive manufacturing.

Although optimization was carried out earlier for this design, there are many manufacturing difficulties in the production of it. Since the load-carrying features are placed to be able to carry the stresses, many volumes should be subtracted from a big rough part. The dimensions for the EOP of the part are given in Figure 22.

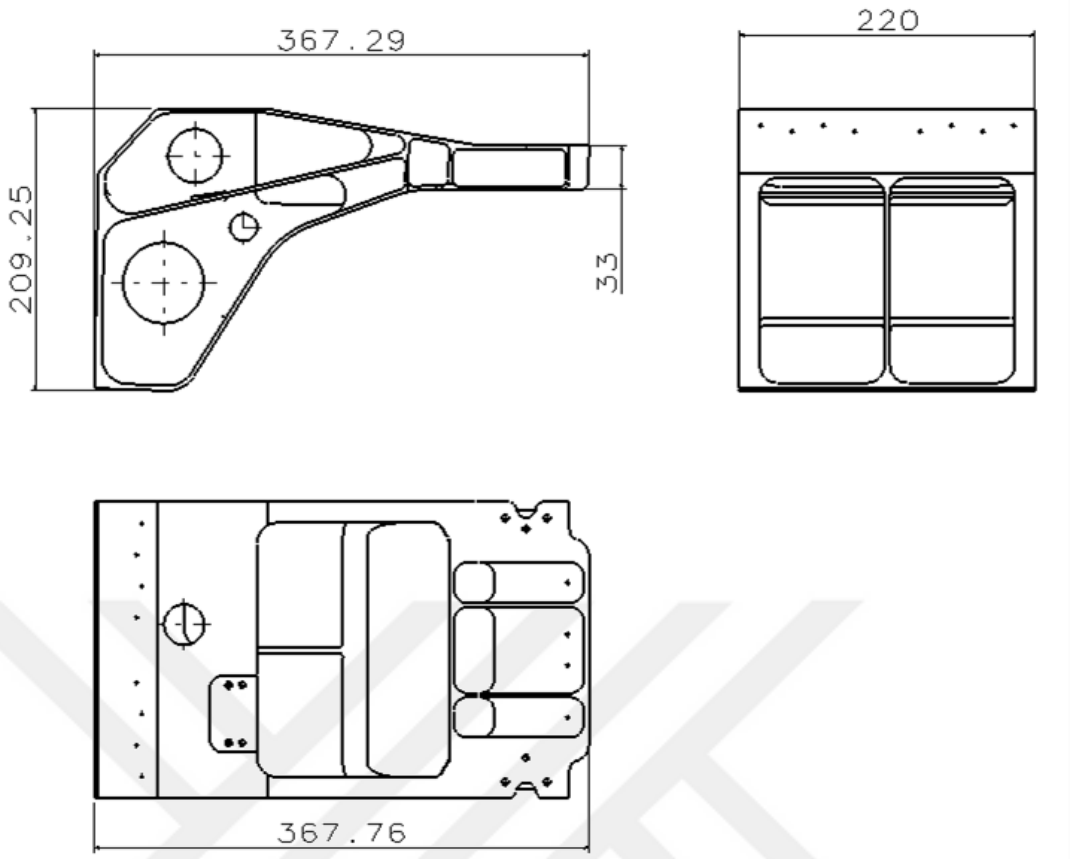

Figure 22: EOP Dimensions of the Part [mm]

3.2 CONSTRAINTS AND LOAD CASES

Before the optimization process begins, constraints and loads must be evaluated and applied because other following steps will be done according to these first inputs. As mentioned before, the relevant part is supposed to carry a component that has approximately 12 kg and the only load that will be applied is the inertia forces of this component. Detailed load explanations will be given in the following sections.

On the other hand, constraints can be divided into two categories: manufacturing constraints and analysis constraints. The basic manufacturing constraints described in Section 2.3.1 will also be applied to this study to achieve a successful manufacturable design.

3.2.1 Manufacturing Constraints

As explained before, owing to nature of the additive manufacturing there are limitations and constraints. The most important of them are minimum length, connectivity, and overhang. Anisotropy should also be considered but, in this study, isotropic analyses are carried out using minimum allowable values.

Minimum Length

It is recommended that use at least 1 mm as the minimum member size for parts that will be using EBM method. Since the part may be manufactured by using this technique in the future, a minimum of 1 mm should be used. With consideration of surface roughness and post-processing steps, 1.5 mm is chosen as the minimum length.

Connectivity

Since the part may be manufactured using Powder Bed Method, there should not be any closed void elements in the part. To ensure that, after the optimization is carried out each result was analyzed to see if there is such a feature.

Overhang

Although one of the most critical constraints for additive manufacturing is the overhang angle, the powder bed method provides an advantage in minimizing the use of support structures. Since the first trials of optimizations showed that there are no critical features for support structures, the overhang constraint is not implemented in the analyses for optimization. While the manufacturing is carried out in future studies, this constraint may be taken into account in case of production trouble.

3.2.2 Analysis Constraints

Space is a very important issue while designing a part for any kind of aircraft. Since the increase in the volume means an increase in mass, designs should be done considering this constraint. In addition to that, there is a very limited area in an aircraft because of all the other system components. So, the dimensions of the newly optimized part should not exceed the values which are given in Figure 22.

In addition to EOP constraints, there must be a certain volume that should not be filled with material in optimization because the system component that will be fastened to the optimized part has a feature consisting of cooling fins. There is a requirement that states there should be a minimum distance between these fins and the supporting structures. In Figure 23, the blue feature shows the volume that must be avoided.

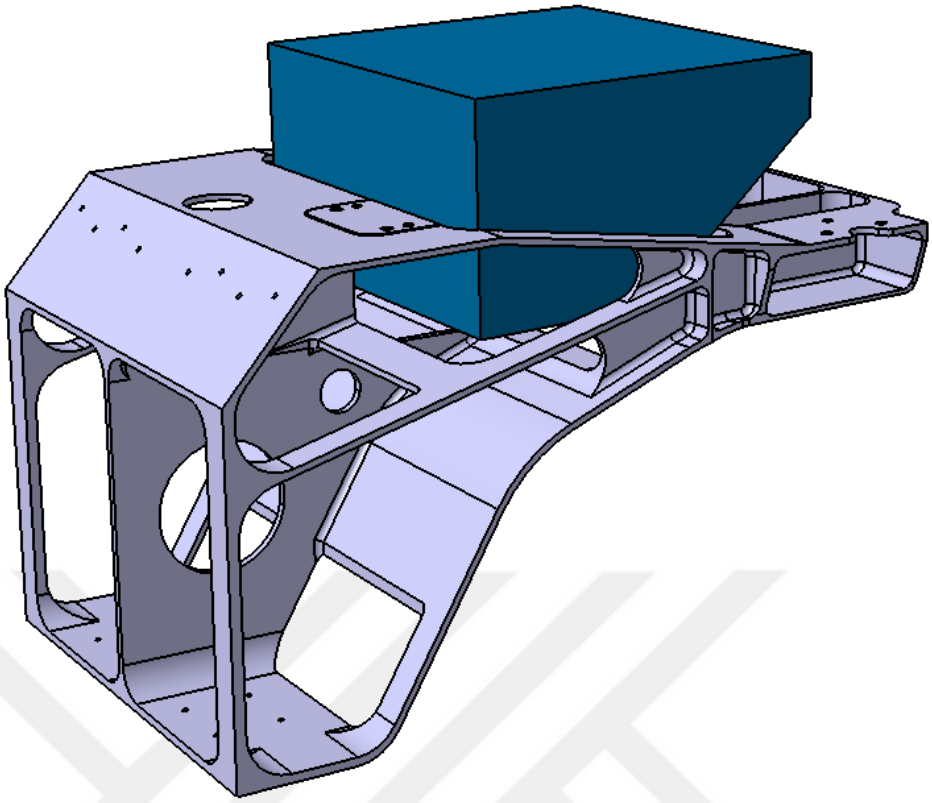

Figure 23: Volume Constraint of the Part

The fastener locations between the aircraft structure and the support part will be the joint constraints in ANSYS Mechanical. Since the support is a structural part there is no need for removal operations so, all the fasteners can be selected as permanent joints like rivets and hi-loks.

To ensure that there will be no fail, fastener analyses should also be done but in this study, the only objective is to achieve an optimized part and make a comparison with the old design. Fastener locations and numbers are also related to the other analyses so all the fasteners are considered as rigid elements which has no deformation. There are also fasteners between the support part and the system component, but they will also not be analyzed in this study.

In Figures 24 and 25, the green surfaces are the connection interfaces of the system component that the optimized part should carry. The fasteners will be placed in the holes on these green surfaces. These surfaces must be in complete flush contact because of the electrical bonding so, there is a surface requirement that should be considered in optimization analyses. While the optimization is carried out, these surfaces must be kept.

The red surfaces are the aircraft structures that can be used to fix the optimized part. Therefore, these surfaces also indicate the outer volume limits.

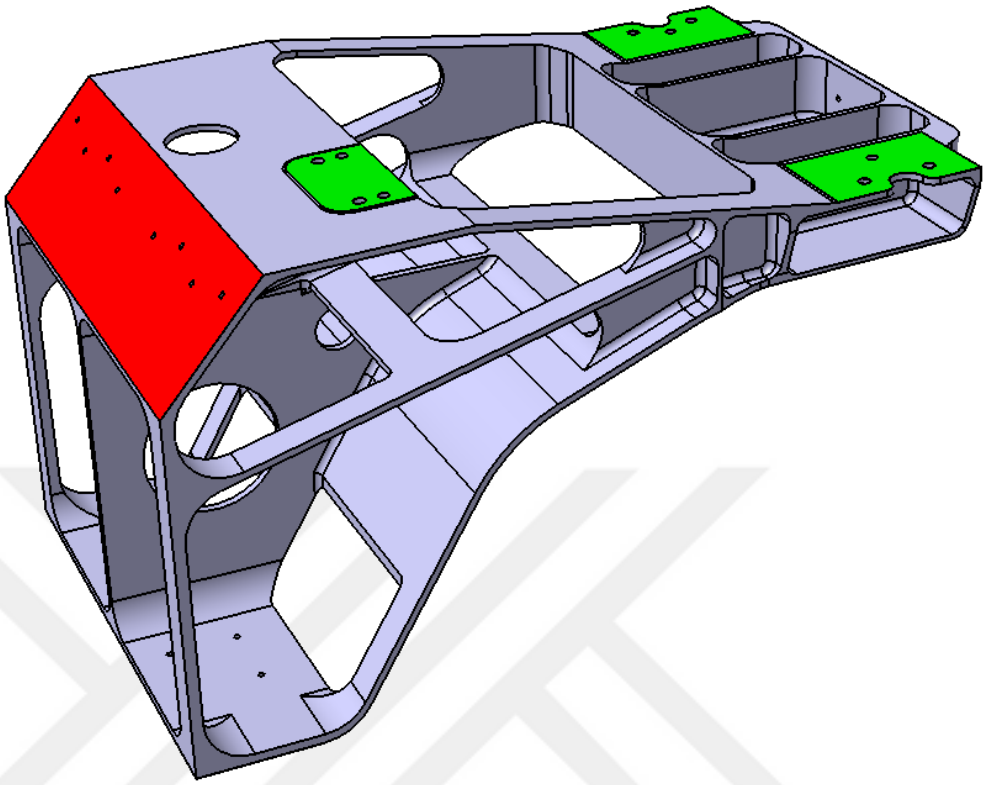

Figure 24: Joint Interfaces of the Support from Top View

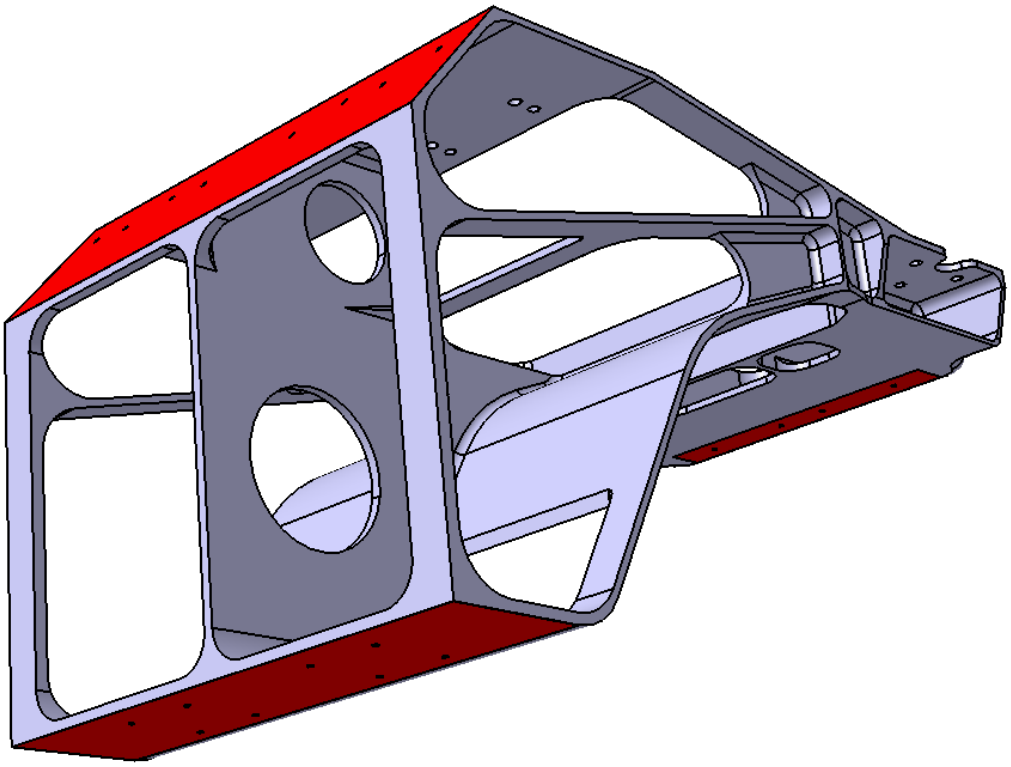

Figure 25: Joint Interfaces of the Support from Bottom View

3.2.3 Loads

As mentioned before, the only load which will be applied is the inertia load of the system component with a mass of 12.65 kg. Inertia load refers to the resistance of an object to a change in its state of motion. It is determined by the object's mass and its distribution around its axis of rotation. When a change in force is applied to the object, such as during a change in speed or direction, the object's inertia causes it to resist the change in motion and maintain its current state. The inertia force can be calculated as follows.

$$F = m\ x\ g \tag{3.2}$$

Where m is the mass of the object in kilograms and g is the acceleration of the object in (m/s^2).

During severe maneuvers, the g forces increase up to 7 – 8g. It means that in a normal state when there is no motion, the earth's gravitational acceleration is considered as 1g but for an aircraft, there may be extreme motions that increase the gravitational acceleration.

The structural analyses are carried out for extreme conditions according to aviation regulations. Although forces are calculated as a result of flight loads, there may be another case that might result in higher forces than flight loads like a crash or collision. For this reason, g values are taken as shown in Table 2 in accordance with aviation standards.

Table 2: G Values of the Analyses

Direction	**X**	**Y**	**Z**
G Values	-30.11	3.18	-5.00

According to these g values, corresponding forces in 3 directions are given in Table 3 by using Equation 3.2. Since these forces are the inertia forces, all of them are implemented from the CoG of the system component as shown in Figure 26.

Table 3: Inertia Forces with Corresponding G Values in Different Directions

Direction	**X**	**Y**	**Z**
Forces [N]	-3736	395	-619

The distances of the system component's CoG (which is the center of the forces) are 313.247 mm in x, 111.043 mm in y, and 336.442 mm in z directions from point O as shown in Figure 26.

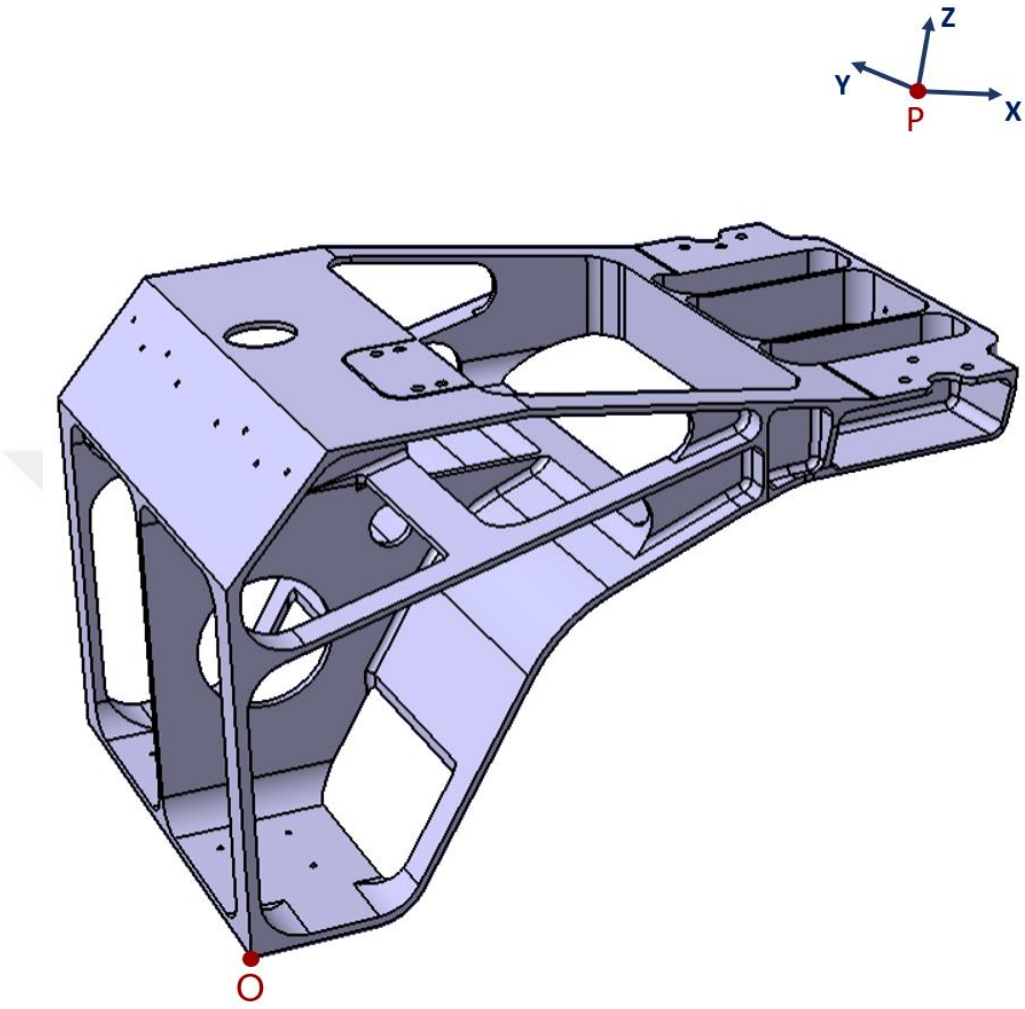

Figure 26: Optimization Part and The Force Center

3.3 VERIFICATION OF CURRENT PART

Before the optimization analyses, a structural analysis of the current part is carried out to verify the part. Comparisons were then made between this analysis and previous studies to ensure that the results are the same.

3.3.1 Material

The material of this current part is Aluminum 7050 T7451. The properties of the material are given in Table 4 according to MMPDS. Since the main requirement states that, '*The part should not fail under the most extreme loading condition*' the safety factor and optimization analyses are carried out with considering the UTS (Ultimate Tensile Strength) of the materials.

Table 4: Material Properties of AL 7050 [49]

Density [kg/m^3]	Tensile Yield Strength [MPa]	Tensile Ultimate Strength [MPa]	Young's Modulus [GPa]	Poisson's Ratio
2820	434	489	71	0.33

3.3.2 Analyses

With using defined values, static structural analysis is carried out. ANSYS Mechanical is used, and the results are given in Figure 27 and Figure 28.

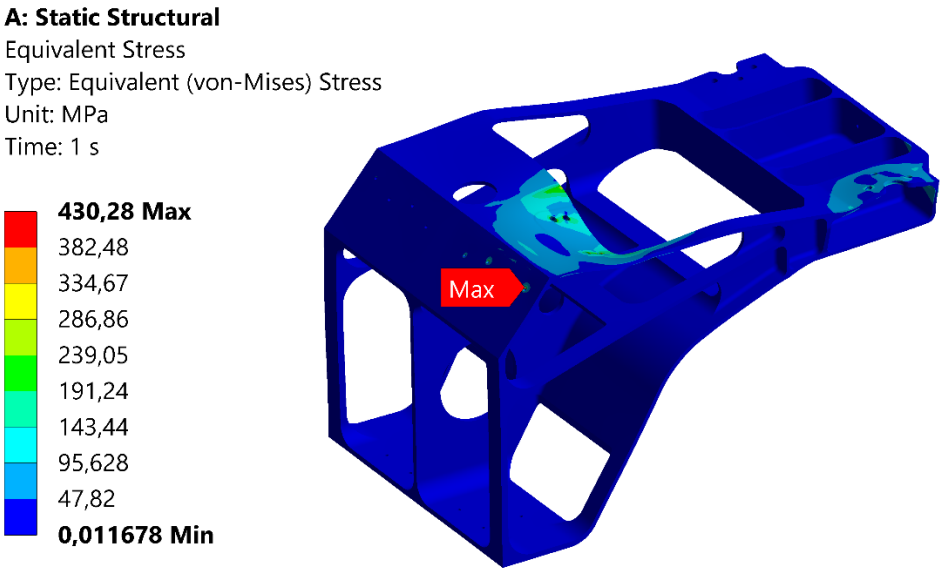

Figure 27: Maximum Von-Mises Stress of Static Structural Analysis

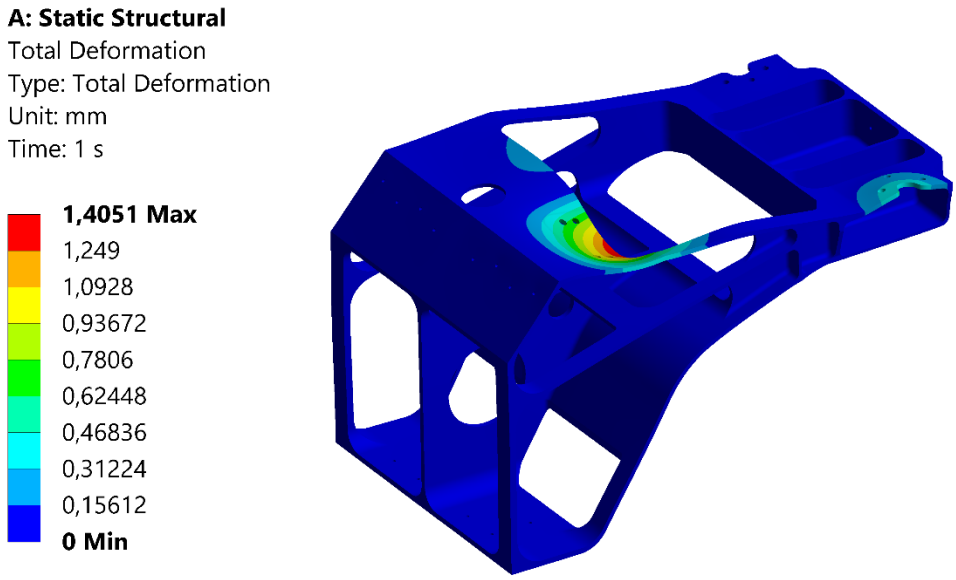

Figure 28: Total Deformation of Static Structural Analysis

Max stress is 430 MPa which provides min. safety factor of 1.137 as shown in Figure 29.

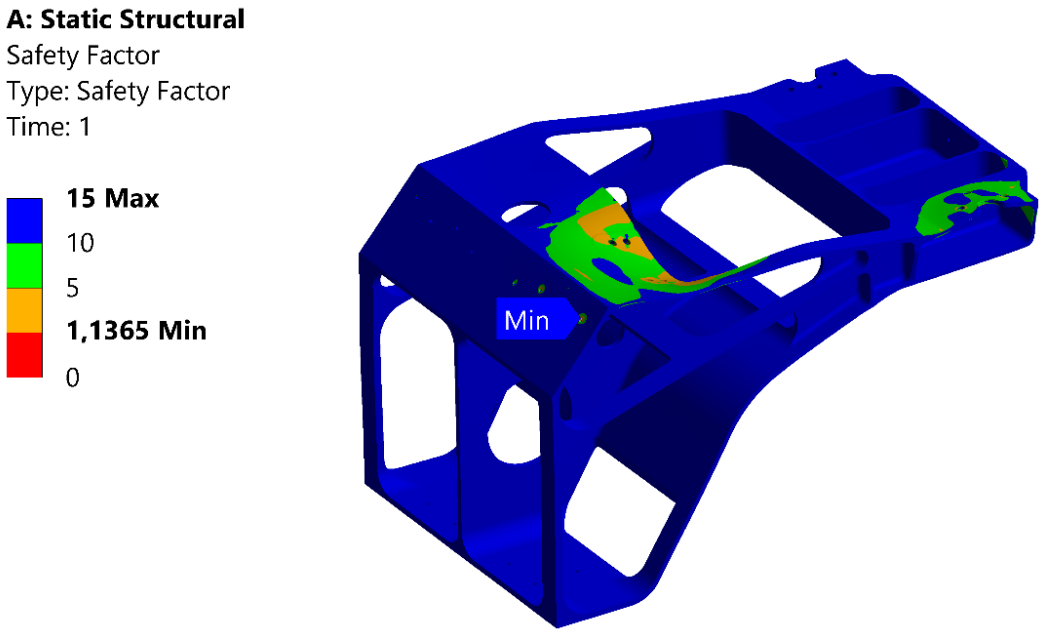

Figure 29: Safety Factor of the Analysis

With these results, the part does not fail under all excessive loads. But as mentioned before because of the manufacturability difficulties and inappropriate stiffener placement, topology optimization can provide better and lighter designs. It can be observed that stresses have occurred in the connection interface between the part and the system component, but there is no feature to avoid stress concentration.

To obtain the proper volume distribution in accordance with the stress concentrations, different design concepts are obtained by using AL 7050 first.

3.4 TOPOLOGY OPTIMIZATIONS AND ANALYSES

Because of the surface requirement which was explained in Section 3.2.2, the connection surfaces must be kept during the analyses.

By the dimensions of the current part, several design options are considered by using a volume as shown in Figure 30. This volume represents the maximum space that can be used for the new part. There is a big gap in the middle of the part due to a feature of the system component which was also introduced in section 3.2.2.

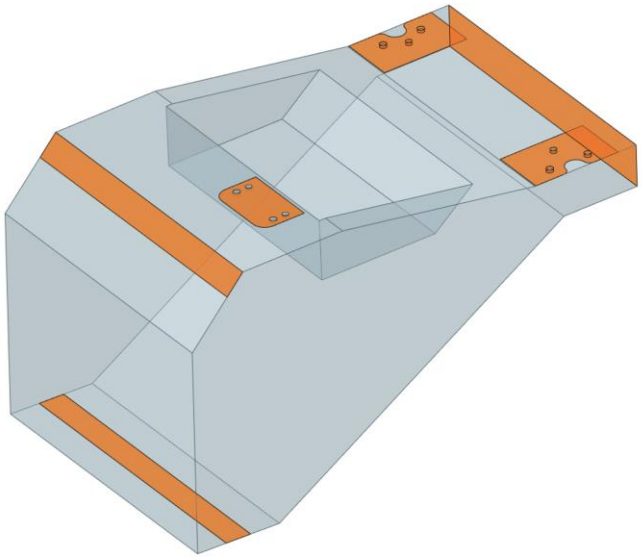

Figure 30: Optimization Volume with All Connection Areas

The highlighted areas are the connection features of the system component and the structure. By using these boundary conditions, 5 different design concepts are considered for obtaining the most efficient material distribution. Mass is selected as the most important criterion for choosing the most suitable concept and all these concepts are obtained by using Ansys Discovery. Since mass is the determining factor, it is set to get 1 as a Safety Factor for all concepts. All concepts are calculated and analyzed in this direction to select the most suitable option in terms of mass.

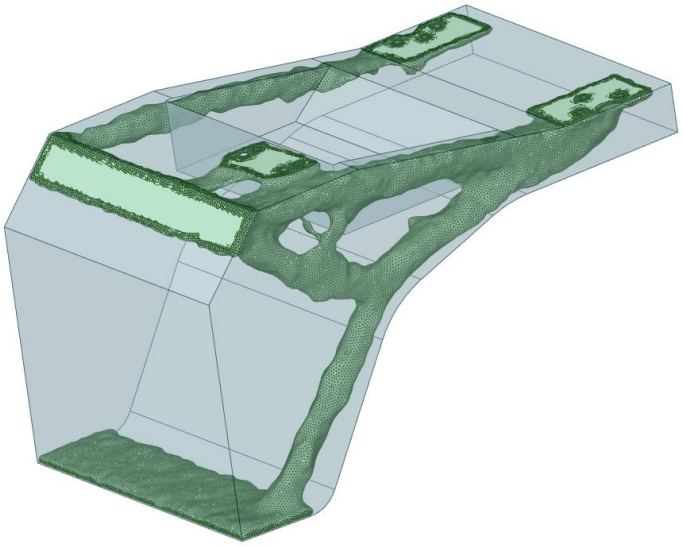

Figure 31: First Design Concept

For the first concept, the bottom and the top connection surfaces are kept, and the resultant part has a mass of 1.716 kg as shown in Figure 31. Since the structural

boundary conditions are selected as explained, the part has features of more than 45-degree inclination according to the bottom or top surfaces. Due to this result, unnecessary support elements will have to be added in the production of the part which is not suitable for the overhang constraint as explained before.

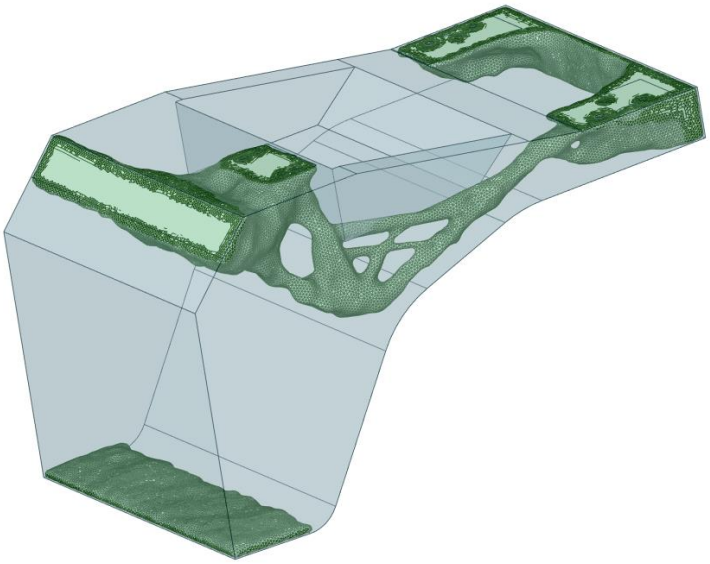

Figure 32: Second Design Concept

For the second alternative shown in Figure 32, the bottom and the front surfaces are determined as structural connection boundaries. In this analysis, it is observed that the bottom surface does not affect the volume of carrying the regarding loads. All the volume between two surfaces is removed in the analysis. The mass for this alternative is obtained as 1.834 kg.

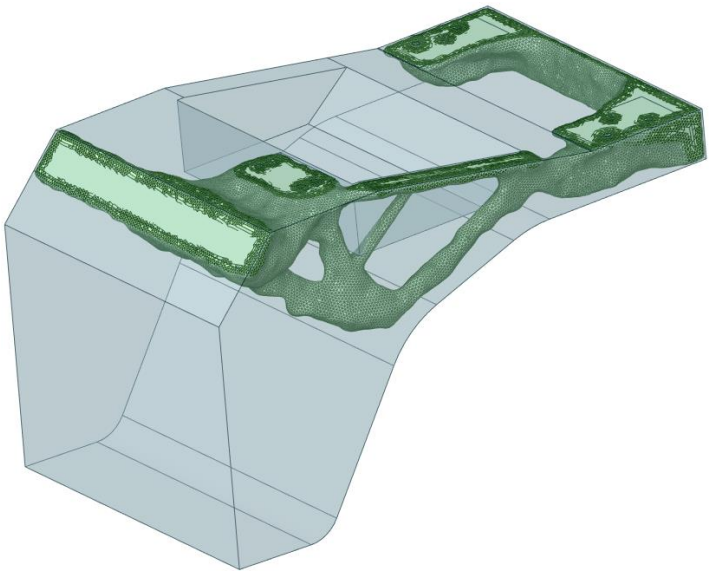

Figure 33: Third Design Concept

After the results in concepts 1 and 2, the bottom surface is not selected. For the structural connections top and front surfaces are kept during the analysis. The part has a mass of 1.608 kg. Even though the overhang for the part is reduced, there are still similar surfaces that are not suitable.

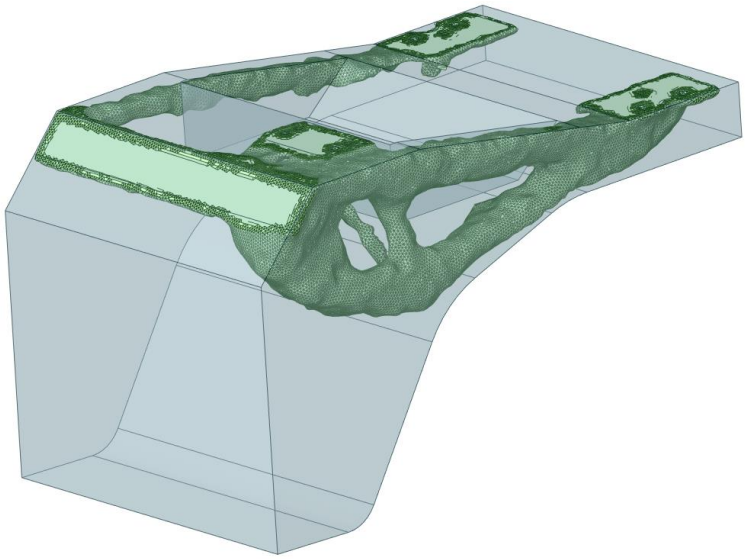

Figure 34: Fourth Design Concept

For this alternative only the top surface is chosen for the structural connection boundary and the mass of the final volume is obtained as 1.286 kg. The best volume for the overhang constraint is achieved with this concept. Also, the mass of the part is reduced more than in other alternatives.

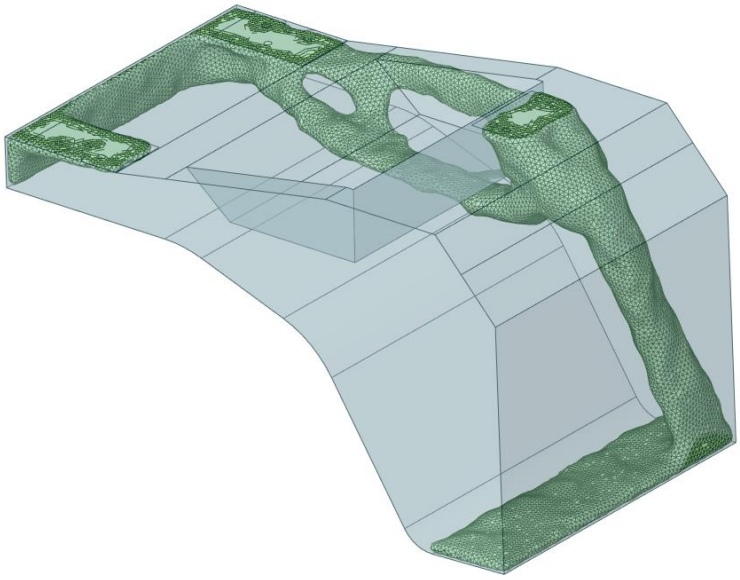

Figure 35: Fifth Design Concept

For the final concept, the front and bottom surfaces are kept during the analyses and the resultant volume has a mass of 1.464 kg. Although the mass is significantly reduced, some features are hard to be manufactured because of the same reasons as Concept 1.

After obtaining all these alternative design solutions, a comparison is made between them for selecting the most suitable boundary conditions in the following analyses and studies. The final masses of these volumes are given in the table below.

Table 5: Mass of the Different Concepts

Concept	**1**	**2**	**3**	**4**	**5**
Mass [kg]	1.761	1.834	1.608	1.286	1.464

According to the mass values and the volumes, it is observed that the bottom connection surface acts like an additional boundary condition. Alternatives without this area have lighter volumes also, from the manufacturing perspective, it is difficult to produce these large volumes stacked on different surfaces in one part.

Considering all the results, the most suitable concept is chosen as 4 because it is the most appropriate alternative for both manufacturing and mass criteria. All the optimization analyses and other studies are carried out in this direction.

The optimization and the result verification analyses are done by using ANSYS Mechanical and the Optimization Type is set to 'Density Based'. The response constraint is selected as mass because the main aim of this study is to reduce the weight of the initial part. It is defined as an 'Absolute Constant' with a maximum value of 1.3 kg firstly to show there is a chance for a reduction in mass around %25 of the part compared with 1.712 kg which is the mass of the current part. The Objective of the analyses is set for minimizing Compliance.

3.4.1 Optimization By Using AL 7050

As explained before, the first optimization is carried out by using AL 7050 as material. The optimization constraints and the material properties were defined in sections 3.2 and 3.3 before. Figure 36 shows the final volume after the smoothing is done by using SpaceClaim.

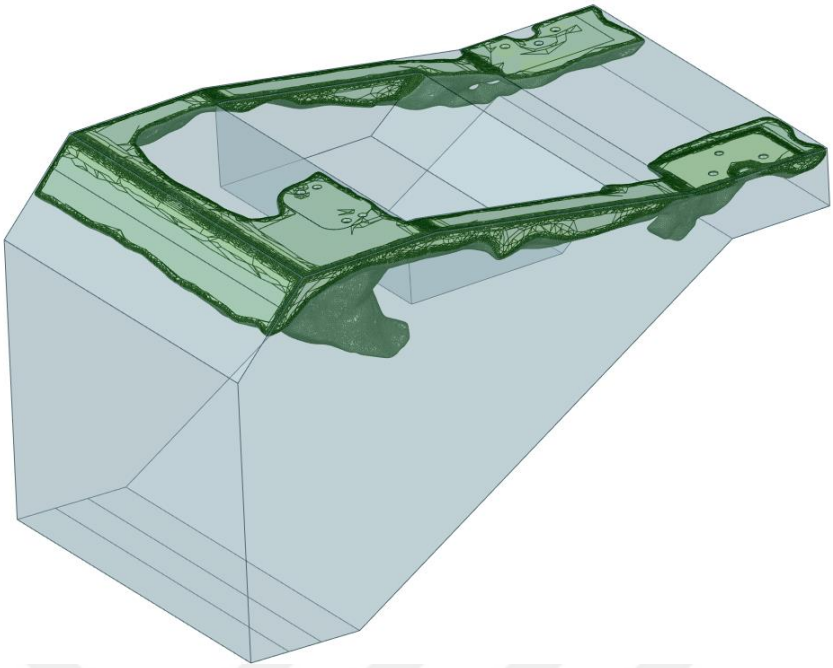

Figure 36: Optimization Result for AL 7050

Smoothing is an important step for optimization because there are many discontinuities and sharp edges in the optimized volume. Therefore, verification analyses should be carried out for smoothed volume. The verification results for AL 7050 analyses are shown in the below figures.

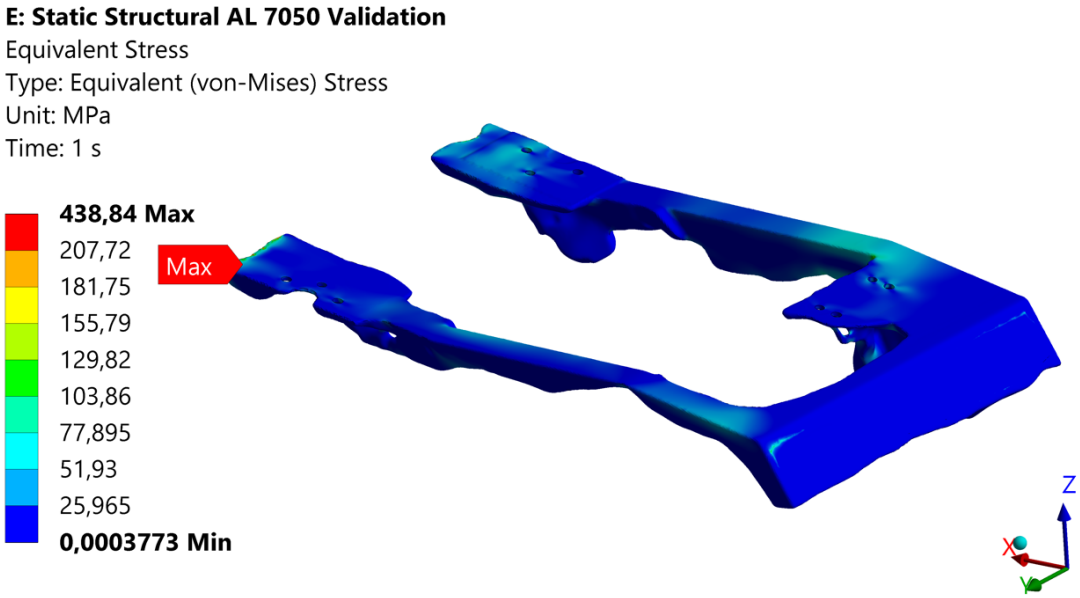

Figure 37: Maximum Von-Mises Stress of Optimized Region for AL 7050

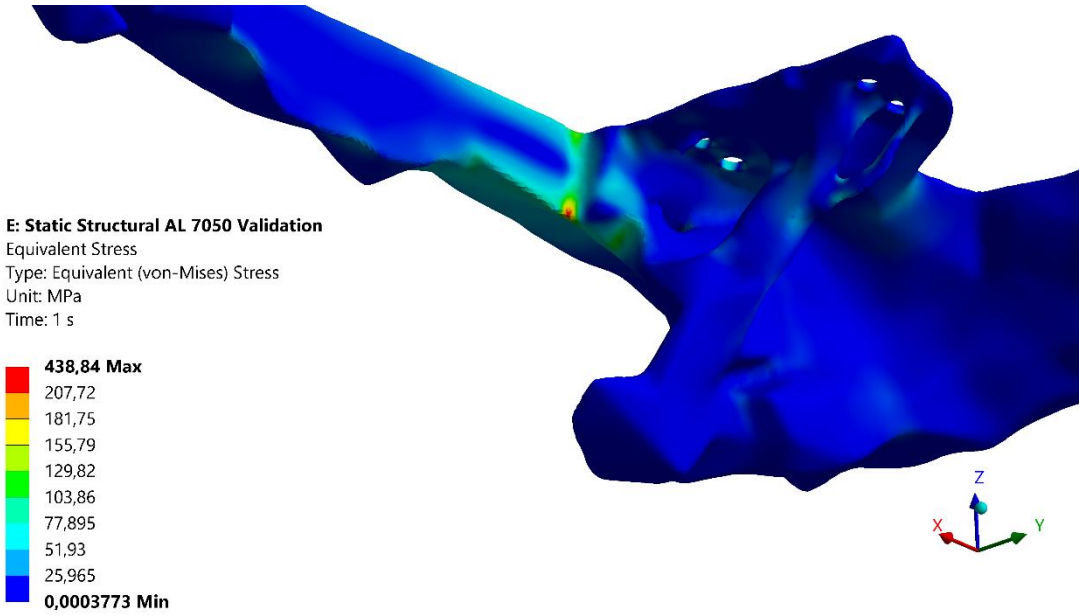

Figure 38: Von-Mises Stresses of Optimized Region for AL 7050

As shown in Figure 37, the maximum stress occurs on the constraint region for the structural connection area, and it is below the UTS of the material which is 489 MPa. It is important to show that there is a stress concentration on the corner of the subtracted volume, but it is also below 489 MPa. The Safety Factor result is shown in the below figure by the von-mises stresses.

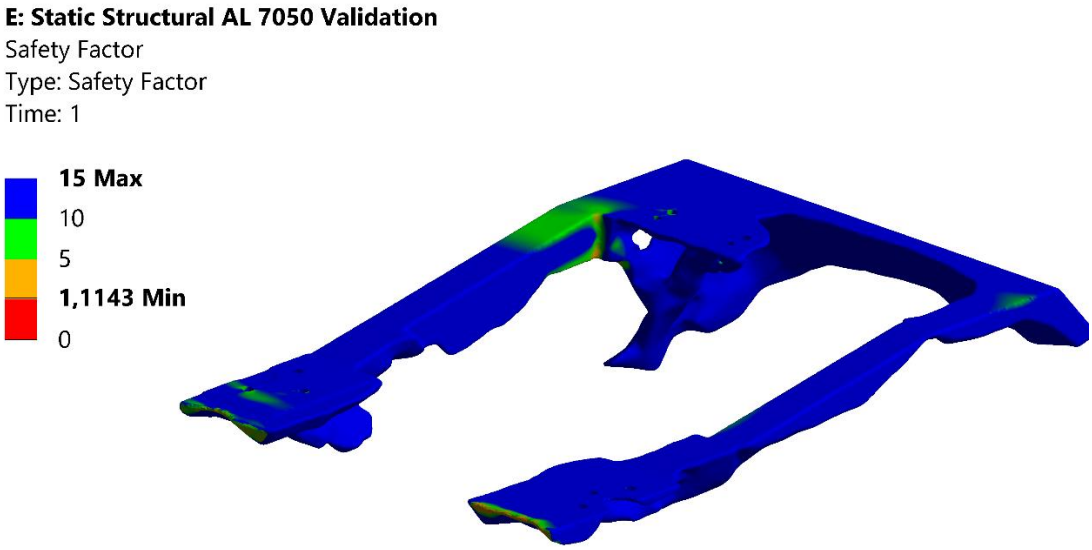

Figure 39: Safety Factor of Optimized Region for AL 7050

It is understood that the optimized part can carry the loads as minimum SF is obtained as 1.11. The mass of the final part is 1.157 kg so there is a 0.550 kg reduction in mass which has a big importance in the aviation industry.

According to these results, the mass of the selected part can be reduced by optimization analyses. So, the analyses are continued using additive manufacturing materials such as Ti64 and AlSi10Mg. The reason for selecting these two materials is their availability in the market.

AlSi10Mg has similar properties and characteristics to AL 7050 so it is expected that there will be no significant difference between these two materials. But, Ti64 has different properties and there is a big difference between Tensile Strengths. For this reason, the study is continued for the results that will be obtained when Ti64 is selected as the material.

3.4.2 Optimization By Using Ti64

Ti6Al4V is a form of titanium (Ti) alloyed with aluminum (Al), vanadium (V), and other minerals. This alloy is particularly popular in the aerospace, medical, and automotive industries because of its lightweight, high strength, and corrosion resistance. The lightweight and durability of Ti6Al4V (usually Ti64) make it an ideal choice for airframes, engine parts, and other structural components. Thanks to its high heat resistance, it can also be used in high-temperature environments such as jet engines. Combined with additive manufacturing, these properties of Ti6Al4V make the material an ideal option for producing complex geometries and customized parts. This is particularly advantageous for single-piece or small-volume production needs.

As mentioned before, Yiğitbaşı S. [43] studied the mechanical properties of Ti64, and the results were given in Table 1 there are more studies in the literature. One of the most significant studies is done by the National Aeronautics and Space Administration [50]. The samples are manufactured by using EBM method and the experimental results for tensile properties are given in Table 6.

Table 6: Experimental Tensile Properties [50]

Sample	Build	E_Z, GPa	Proportional limit, MPa	0.02% yield, MPa	0.2% yield, MPa	Ultimate strength, MPa	Failure strength, MPa	Failure strain, percent	RA, percent
–196 °C									
25	1-1-2	129	1530	1534	1702	1744	1671	10.9	20
43	1-1-2	126	1582	1582	1696	1731	1695	8.1	13
105	1-2-2	126	1579	1583	1695	1733	1682	9.8	17
122	2-4-1	124	1407	1416	1555	1608	1607	5.8	6.5
170	2-4-5	121	1452	1455	1549	1605	1565	12.2	18
191	2-4-9	120	1478	1478	1589	1646	1633	8.8	12
–101 °C									
28	1-1-1	128	1272	1283	1336	1394	1289	14.0	26
55	1-1-4	124	1243	1258	1324	1387	1301	14.3	22
95	1-2-2	127	1266	1276	1339	1406	1356	12.4	19
147	2-4-3	121	1180	1187	1243	1300	1274	13.1	18
160	2-4-4	119	1191	1196	1237	1287	1238	13.7	22
198	2-4-8	122	1117	1160	1244	1304	1208	15.7	27
20 °C									
16	1-1-2	125	------	------	------	------	------	------	------
65	1-1-4	124	974	998	1028	1126	1000	21.5	30
67	1-1-4	122	980	1000	1025	1122	998	21.0	31
115	1-2-1	126	967	992	1024	1140	1014	20.7	30
135	2-4-2	118	908	929	960	1042	962	20.2	28
173	2-4-6	118	914	935	965	1051	960	20.7	29
186	2-4-6	118	928	941	972	1048	1027	9.8	11
H1	------	118	865	896	958	1058	970	13.6	12
H3	------	119	831	866	950	1057	992	13.2	14
H11	------	118	866	901	977	1081	1064	14.4	13
149 °C									
34	1-1-2	118	745	788	813	948	676	18.1	49
78	1-1-3	117	768	798	819	941	627	22.0	55
86	1-2-2	117	792	804	817	944	834	18.2	43
141	2-4-1	111	701	722	747	841	576	22.0	58
153	2-4-5	113	689	730	760	854	753	17.1	50
183	2-4-9	113	729	749	775	861	540	21.1	39

Also, in a study of Manikandakumar Shunmugavel, Ashwin Polishetty, and Guy Littlefair [51], the mechanical properties of Ti64 manufactured by SLM method are given in Table 7.

Table 7: Tensile Properties of the Tested Bars [51]

Material	**SLM Ti-6Al-4V (Longitudinal)**	**SLM Ti-6Al-4V (Transverse)**
Young's Modulus [Gpa]	113	109
Yield Strength [Mpa]	964	1058
Ultimate Tensile Strength [Mpa]	1041	1114
Percentage of Elongation [%]	7	3
Percentage of Reduction in Area [%]	13	11

One of the largest AM printer manufacturers EOS has also studied the mechanical properties of Ti64 by their printers. The company also provides AM powders and the properties are given in Table 8.

Table 8: Mechanical Properties of Ti64 Provided by EOS [52]

Material	**Ti-6Al-4V (As-built)**	**Ti-6Al-4V (Heat-treated)**
Young's Modulus [Gpa]	110	116
Yield Strength [Mpa]	1060	860
Ultimate Tensile Strength [Mpa]	1230	930
Percentage of Elongation [%]	10	14

As shown in the tables, there are many different values obtained by different studies and companies and these values do not converge on a single value for strengths of Ti64. To be able to preserve the conservative approach, Tensile Strength is taken as 880 MPa and the Ultimate Strength is taken as 950 MPa for the analyses. The density of the material is 4330 kg/m^3 and the Young's Modulus is taken as 113 GPa.

Optimization settings and constraints were kept the same with the AL 7050 analyses. Since the most appropriate concept was determined before, the optimization is carried out in accordance with this alternative. The optimized smoothed volume by the given values is shown in Figure 40.

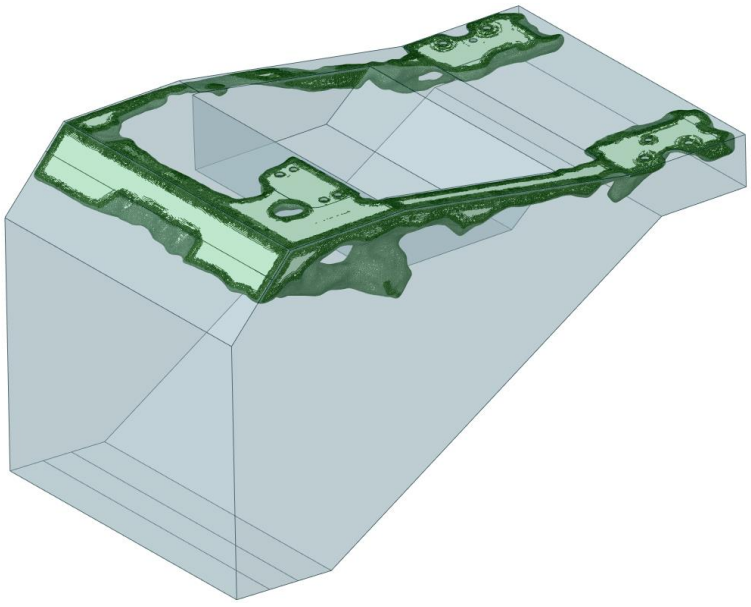

Figure 40: Optimized Volume for Ti64

The structural analyses according to the given loads are given in Figure 41 and Figure 42.

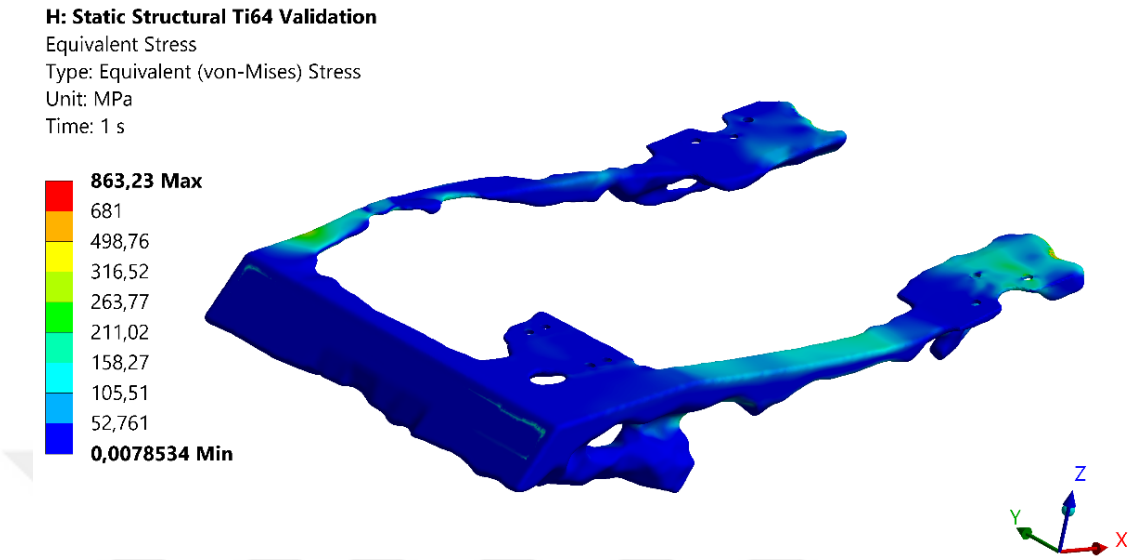

Figure 41: Maximum Von-Mises Stress of Optimized Region for Ti64 - 1

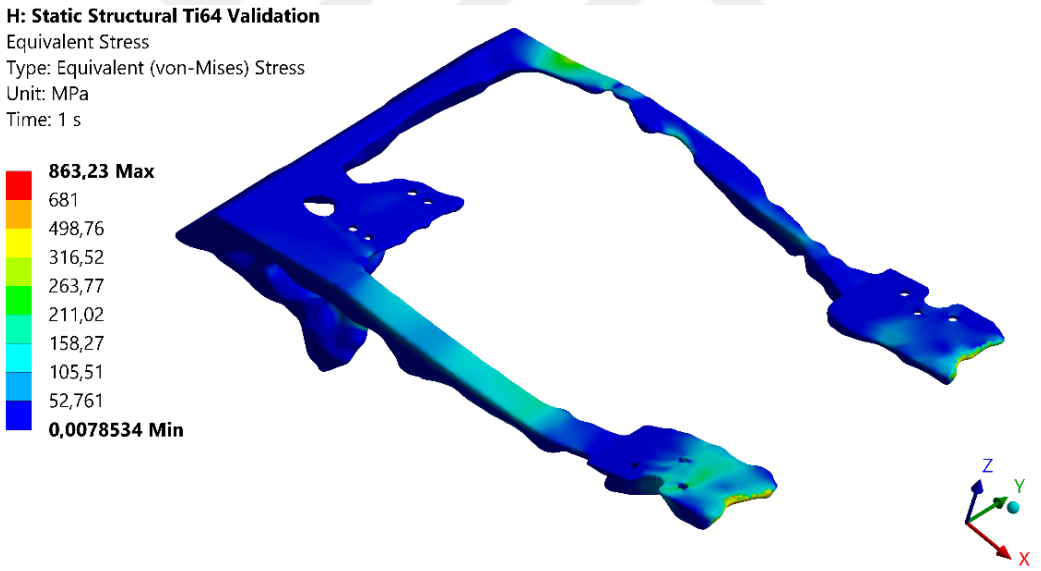

Figure 42: Maximum Von-Mises Stress of Optimized Region for Ti64 - 2

The Safety Factor analysis is also given in Figure 43 for Ti64 according to Ultimate Tensile Strength of the material which was determined as 950 MPa earlier.

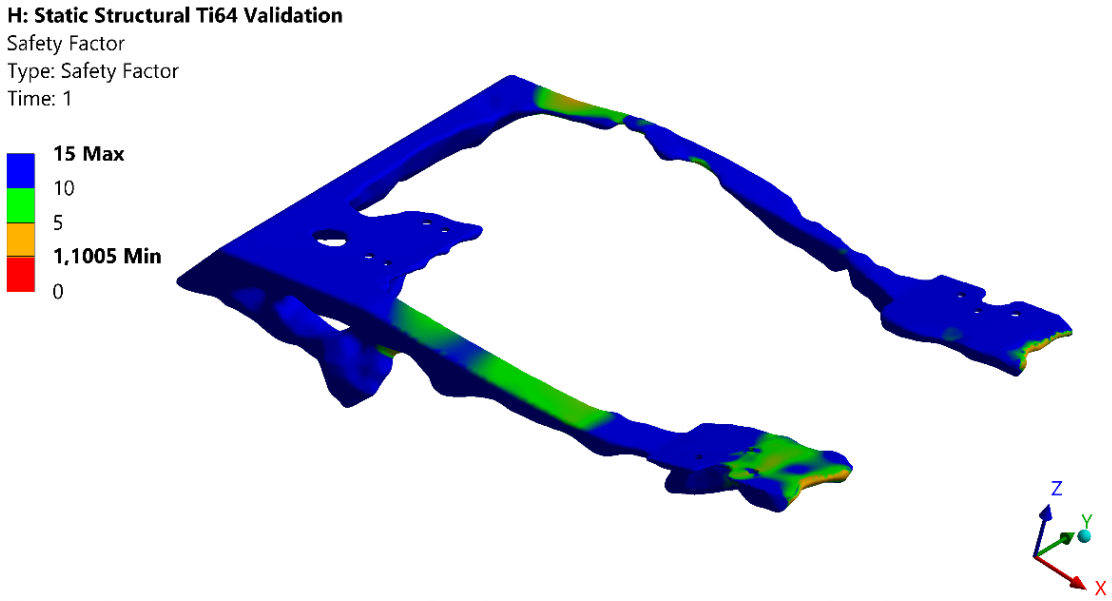

Figure 43: Safety Factor of Optimized Region for Ti64

As shown in Figure 43, the minimum Safety Factor is obtained as 1.10 which means this optimization is also successful. Since the optimization settings are the same as the AL 7050, this optimization ended up with more conservative results because the Ti64 has more stiff properties.

The optimized volume has a mass of 1.375 kg, which means there is a 0.337 kg reduction in mass. The value was 0.550 kg for the Al 7050 but, the final comparison will be done after the analyses are carried out for AlSi10Mg.

3.4.3 Optimization By Using AlSi10Mg

AlSi10Mg is an alloy obtained by mixing aluminum, silicon, and magnesium in certain proportions. This alloy generally contains 90% aluminum, 10% silicon, and magnesium as a percentage. It is used in many applications due to its high stiffness, good strength to weight, excellent thermal conductivity, and low coefficient of thermal expansion.

AlSi10Mg is one of the most preferable materials in industries such as automotive, aerospace, electronics, and machine manufacturing. It is considered an ideal material for additive manufacturing (3D printing) because it has excellent casting properties. The ability to print complex geometries and manage heat effectively makes this alloy suitable for electronic devices and other similar applications. It is widely used in additive manufacturing using metal 3D printing technologies such as Selective Laser Melting (SLM) or Direct Metal Laser Sintering (DMLS).

Much research has been done on the mechanical properties of ALSi10Mg. Since the material is also used in the casting method, many data are available in the literature. However, when additive manufacturing takes place, there will certainly be differences in the properties. One of the most representative studies is done by K. Kempen, L.Thijsb, J. Van Humbeeck, and J. P. Krutha in 2012 [53]. The following table shows the experimental results for samples produced by SLM method.

Table 9: Mechanical Properties of SLM Samples [53]

Material	**AlSi10Mg (XY Direction)**	**AlSi10Mg (Z Direction)**	**AlSi10Mg (Conventional cast)**
Young's Modulus [Gpa]	68	68	71
Ultimate Tensile Strength [Mpa]	391	396	300-317
Percentage of Elongation [%]	5.55	3.47	2.5

In addition to Table 9, Figure 44 shows the Stress-Strain Graph of AlSi10Mg samples which are produced in different directions.

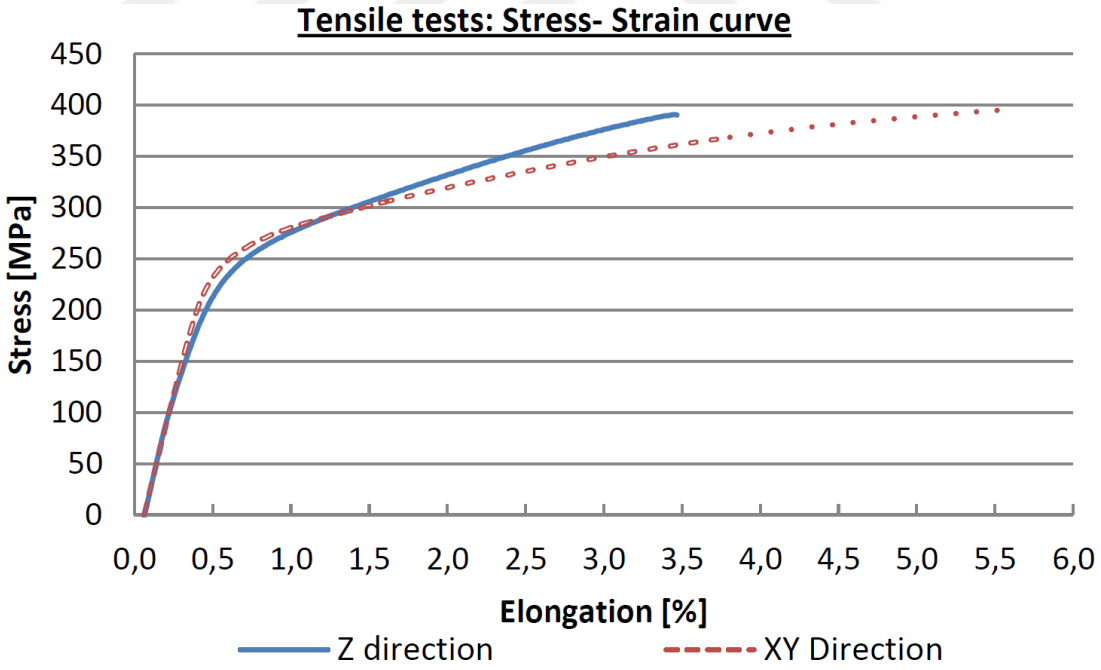

Figure 44: Stress-Strain Curve for Different Directions [53]

As shown in the results, the parts produced by SLM methods have higher UTS than the samples produced by conventional casting. The reasons for this difference are the microstructure and the distribution of the Si phase [53].

EOS has also studied the mechanical properties of AlSi10Mg by using the same procedures as the Ti64 tests. Since the conditions and manufacturing techniques are the same, the comparison between the properties of Ti64 and AlSi10Mg can be made by using their values.

Table 10: Mechanical Properties of AlSi10Mg Provided by EOS [54]

Material	**AlSi10Mg (As-built)**	**AlSi10Mg (Heat-treated)**
Young's Modulus [Gpa]	75	70
Yield Strength [Mpa]	270	230
Ultimate Tensile Strength [Mpa]	460	345
Percentage of Elongation [%]	6	11

Like Ti64, the values do not converge according to the studies and the tests. By using the same conservative approach as before analyses Yield Strength and Ultimate Strength are determined as 230 MPa and 410 MPa respectively. Density is taken as 2680 kg/m^3 and the Young's Modulus of the material is 70 GPa.

Using the same optimization setting and constraints, all the analyses are carried out again. The smoothed final volume after the optimization is shown in Figure 45.

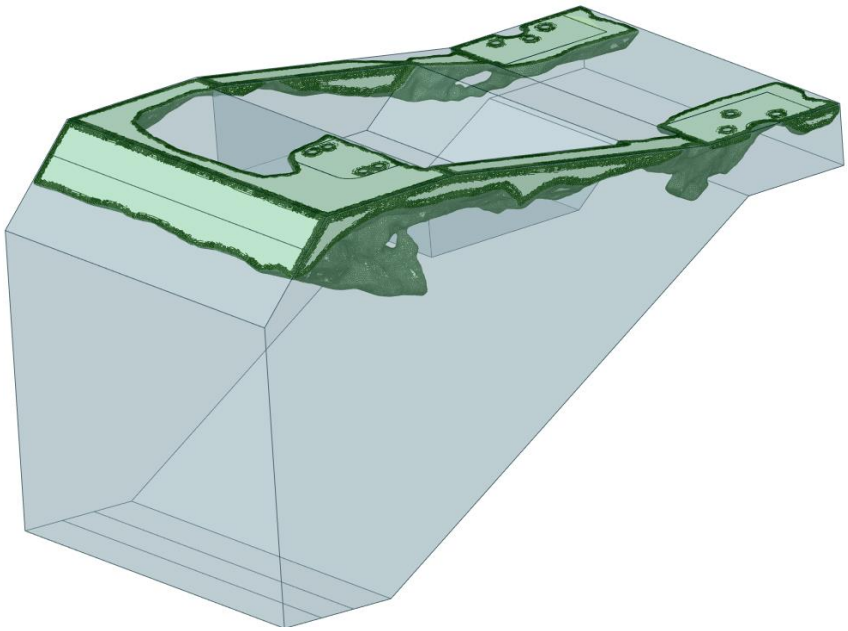

Figure 45: Optimized Volume for AlSi10Mg

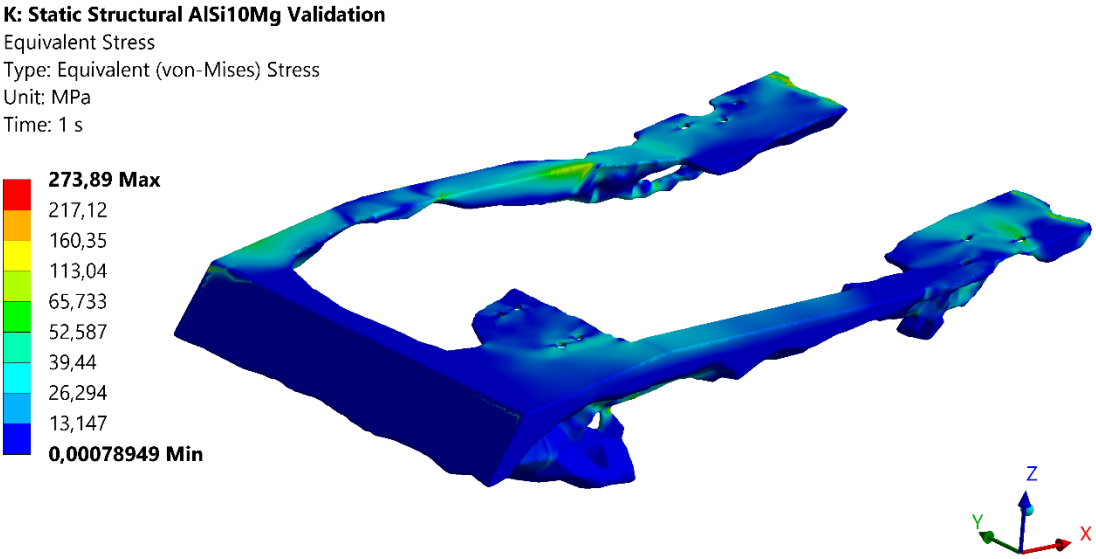

Figure 46: Maximum Von-Mises Stress of Optimized Region for AlSi10Mg – 1

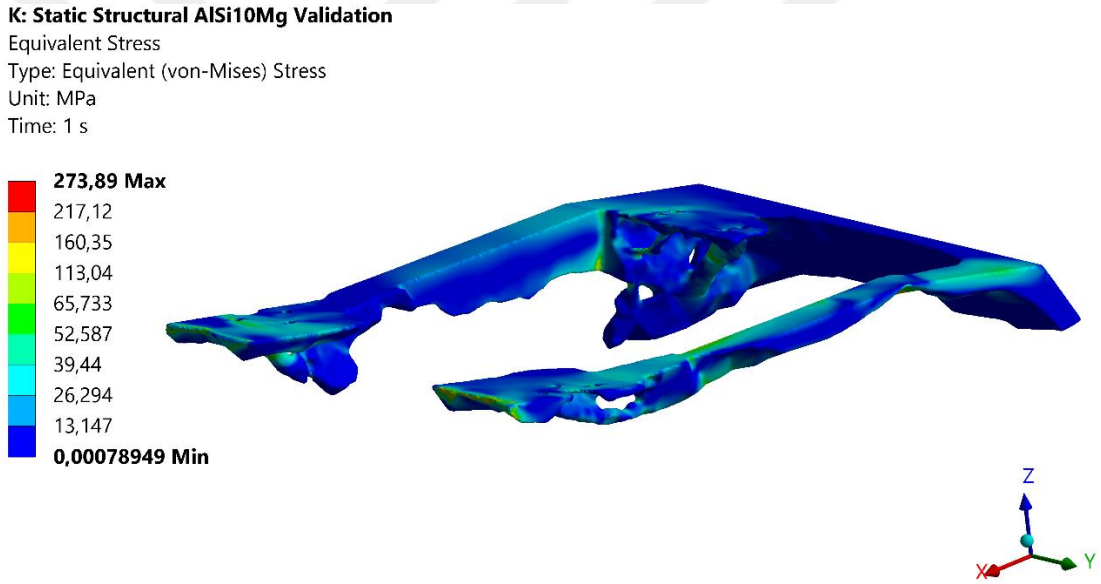

Figure 47: Maximum Von-Mises Stress of Optimized Region for AlSi10Mg – 2

For the aluminum, the minimum Safety Factor is obtained as 1.49 after the smoothing process. The mass of the volume is reduced to 1.058 kg even the highest SF is obtained by comparing the other materials. The part which is in use has a mass of 1.712 kg so almost %40 of the material is removed by performing optimization studies using AlSi10Mg.

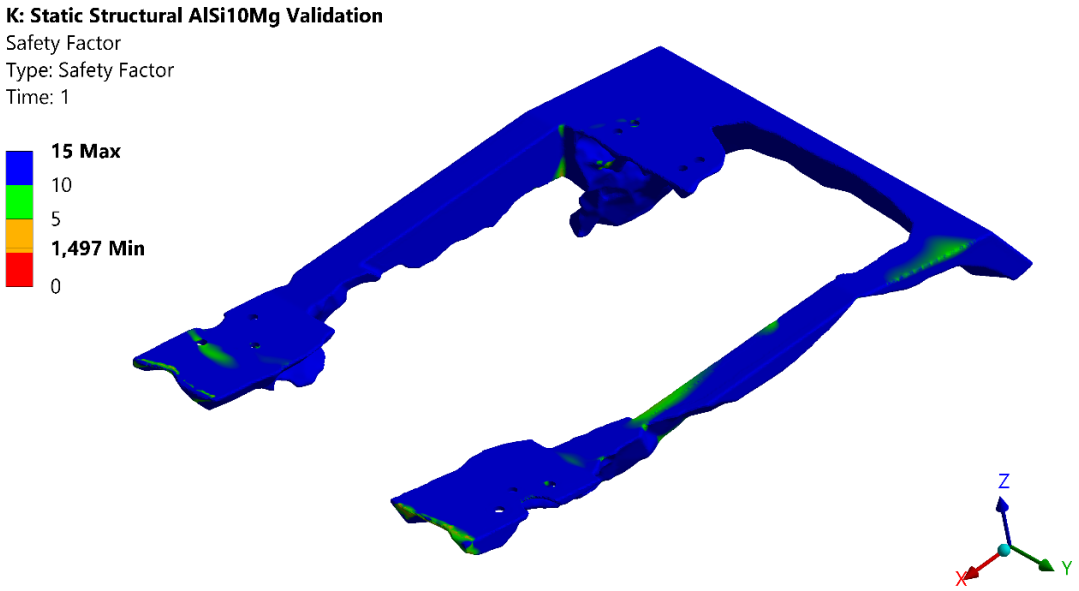

Figure 48: Safety Factor of Optimized Region for AlSi10Mg – 1

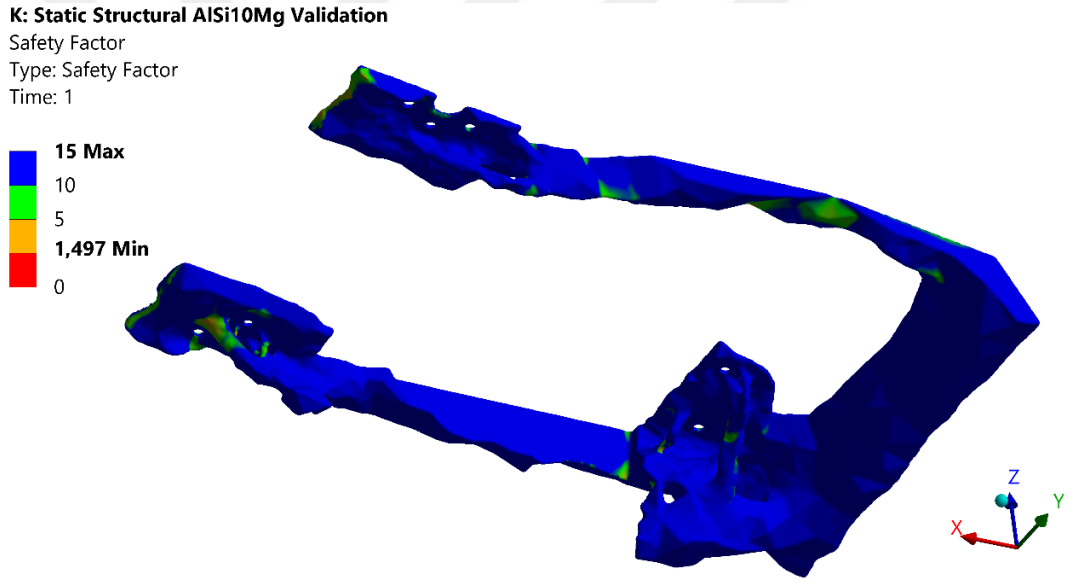

Figure 49: Safety Factor of Optimized Region for AlSi10Mg – 2

3.5 OPTIMIZATION RESULTS

As explained in section 3.4.1, two different materials are studied to be able to choose the proper material for reducing the weight. Firstly, AL 7050 is used for determining the optimization constraints and settings. There have been many analyses using this material since all the conditions should be the same for the next analyses to compare 2 different materials. The results were presented in detail in the previous sections.

After this step, Ti6Al4V and AlSi10Mg were used for the analyses. The results and final masses of the optimized parts are given in Table 11.

Table 11: Results of the Analyses

Material	AL 7050 (Current)	AL 7050 (Optimized)	Ti6Al4V	AlSi10Mg
Safety Factor	1.13	1.11	1.10	1.49
Mass [kg]	1.712	1.157	1.375	1.058
Percent of Mass Reduction	-	%32.41	%19.68	%38.20

Results clearly show that aluminum-based materials are more advantageous in weight than titanium-based materials. In addition to this condition, using aluminum is safer since all the other surrounding parts are made of AL 7050. The mass advantage and avoidance of the risk of galvanic corrosion in dissimilar materials make AlSi10Mg the most suitable material for optimization analyses.

After the material selection, the same steps are taken for considering fastener locations and all the aviation and company requirements to obtain the final manufacturable part. The optimized volume can be seen in the below figures.

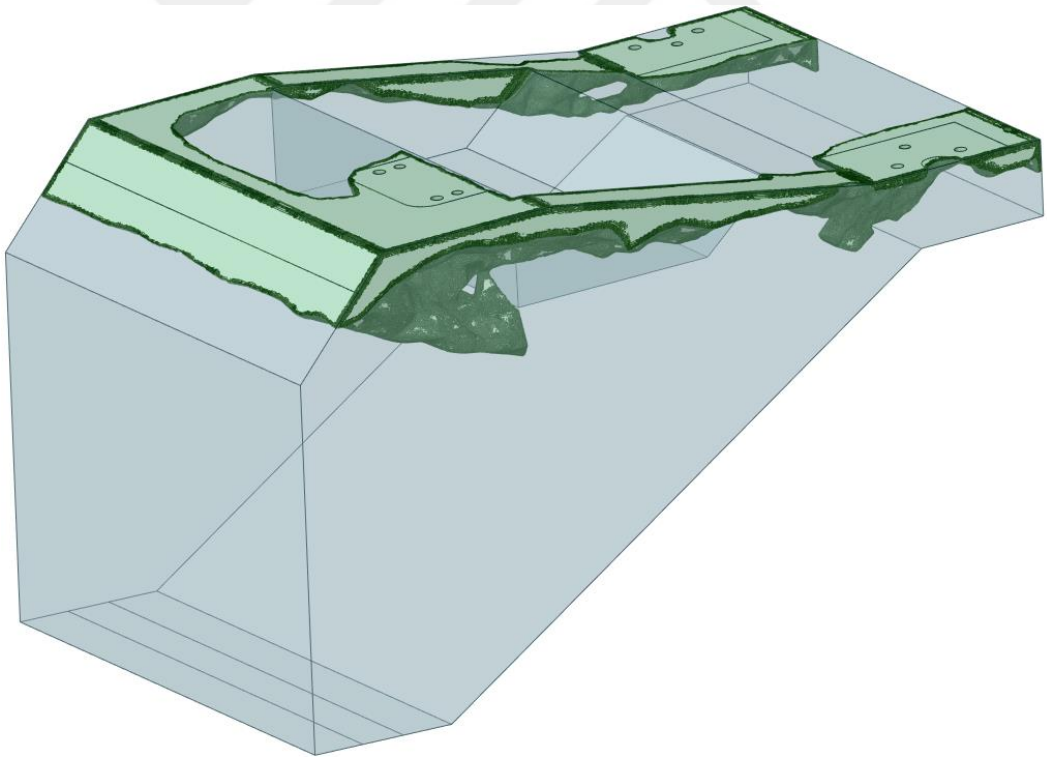

Figure 50: Final Optimized Part from Right

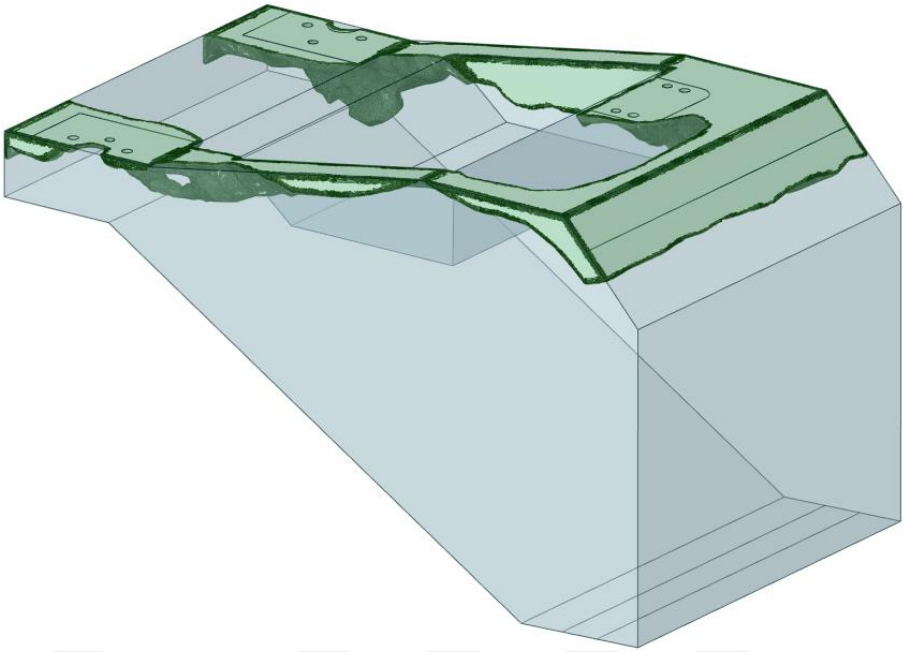

Figure 51: Final Optimized Part from Left

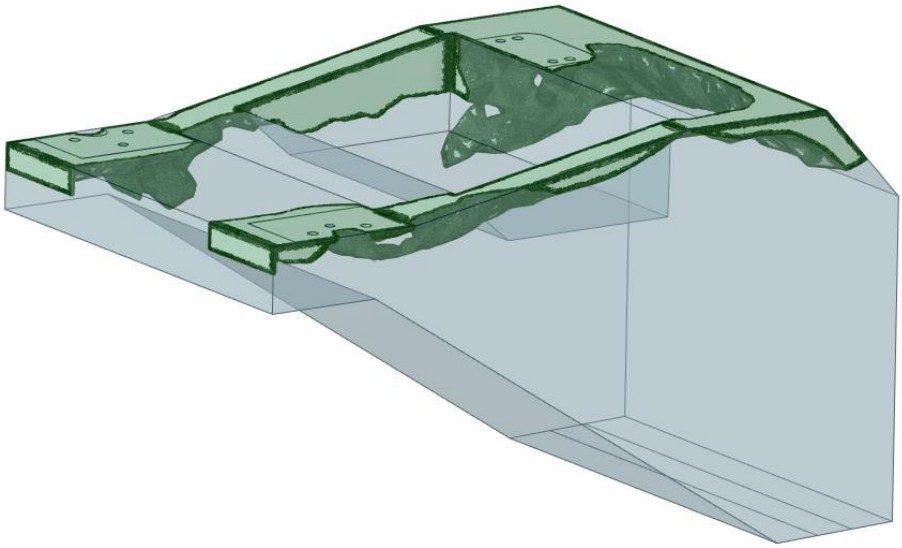

Figure 52: Final Optimized Part from Front

As shown in Figure 52, the connection surfaces are kept flat as possible to get a better bonding area and the load transfer between the fastener and the structure. These surfaces are dimensioned according to structural design criteria such as minimum distance to radius, minimum distance to edge, and minimum distance between the fasteners by fastener diameter.

Also, there are some limitations, which are determined by the manufacturing team and come from the printer like printing direction, infill patterns, etc. Validation analyses for the final part are given below figures.

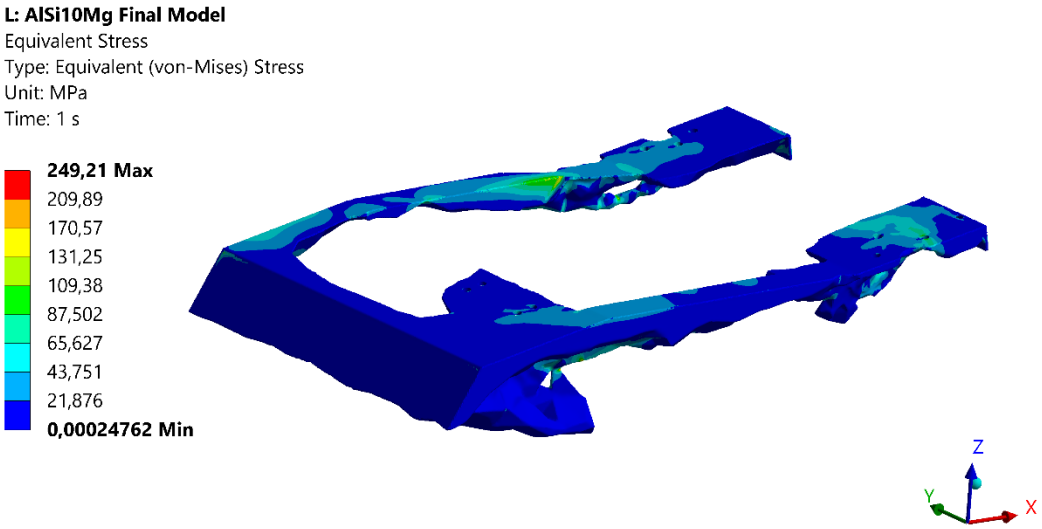

Figure 53: Maximum Von-Mises Stress of Final Optimized Part – 1

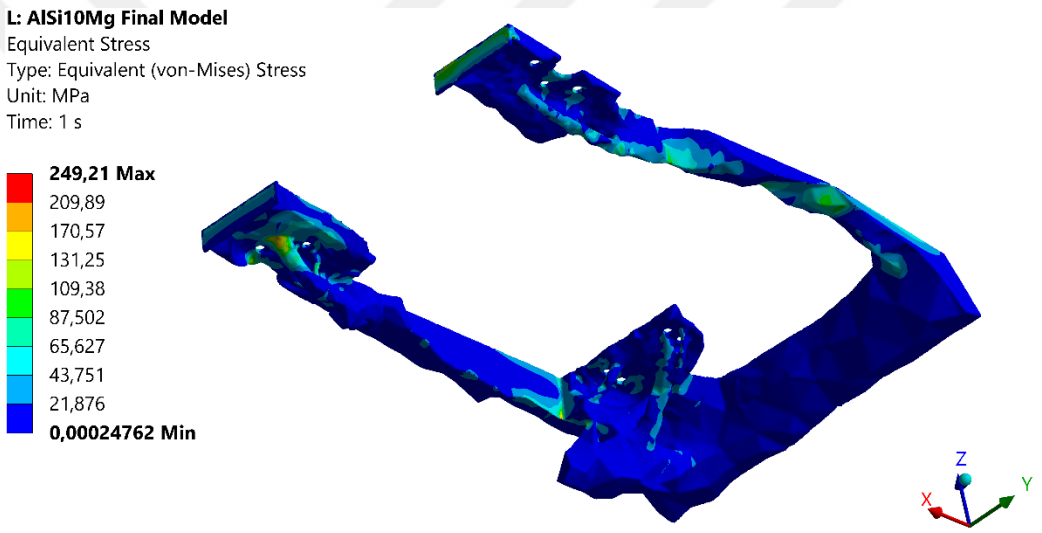

Figure 54: Maximum Von-Mises Stress of Final Optimized Part – 2

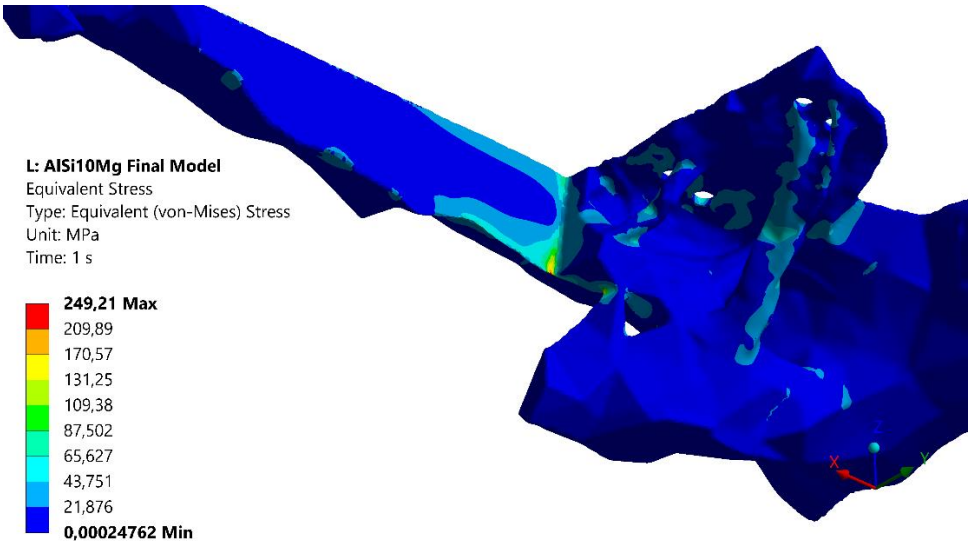

Figure 55: Maximum Von-Mises Stress of Final Optimized Part – 3

In Figure 55, it is seen that there is a stress concentration on the corner of the subtracted volume. The same result appeared in AL 7050 analysis but like before analyses, the stress concentration level is below the UTS of the material.

According to the stress requirements, a minimum level of 1 for the Factor of Safety is a good result, but it is still desirable to maintain levels of 1.5 in the analysis. Because even when all conditions are considered, there may still be missed calculation errors due to the programs. The SF analyses are also given in the below figures.

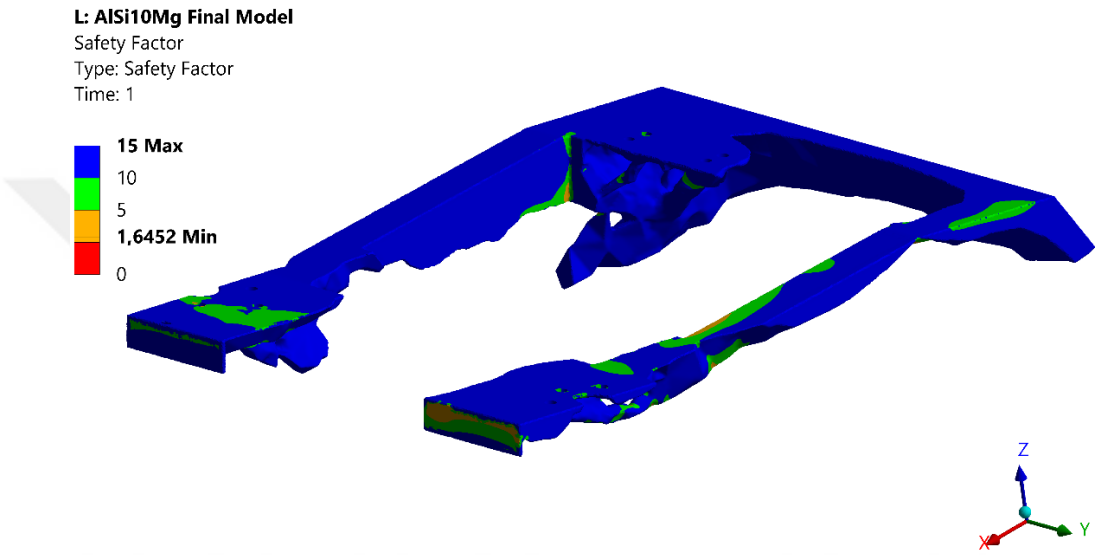

Figure 56: Safety Factor of Final Optimized Part – 1

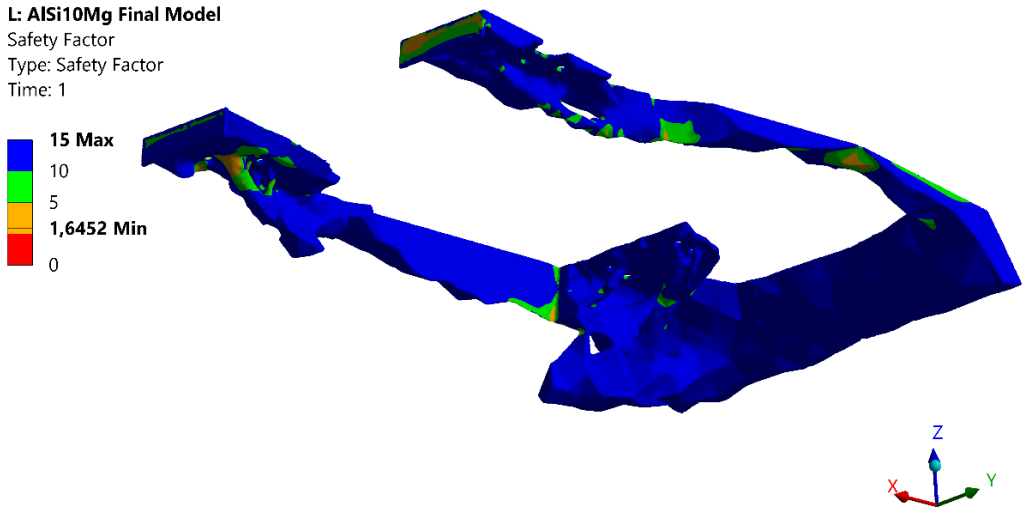

Figure 57: Safety Factor of Final Optimized Part – 2

The minimum safety factor is obtained as 1.65 as shown in the figures. The minimum acceptable value of SF is 1.5 as mentioned before so this result passes all the stress requirements.

CHAPTER IV
ANISOTROPIC TOPOLOGY OPTIMIZATION

Anisotropy can be explained as a change in the properties of a material depending on its orientation. As an example, the strength or conductivity of a material may be different in one direction than in the other. This occurs naturally, for example, in composite materials, natural crystals, and wood, and significantly influences the behavior of the material in engineering applications.

It is one of the most remarkable challenges in topology optimization since the directional dependence of the material's properties can affect the overall performance and efficiency of the design. Due to the layer-by-layer manufacturing technique, the composition of the material in each layer is different from the composition in the regions where the layers meet. This dissimilarity in structure results in various mechanical properties in components produced by 3D printing, creating anisotropic properties. The reason for this dissimilarity can be explained by using Figure 58.

Figure 58: 3D Manufacturing Scheme

Since the production occurs layer by layer, some regions may not melt and solidify within a complete unity as a layer. When the force is applied perpendicular to these regions, the material cannot act as a whole solid so there may be failure in these areas.

The same phenomena can also be shown in composite materials. Since fibers are not capable of carrying load perpendicular to the fiber direction, the staking is done by considering the load path on the part. In 3D printing technology, there is only one direction for manufacturing so, even if the same method cannot be applied, there are many methods to overcome this problem.

4.1 ANISOTROPY OF TI64 IN ADDITIVE MANUFACTURING

Previously, the main studies and examples were given in Section 2.3.1.4, and the tensile test results applied to the samples produced in 3 different directions were given in Table 1 [43]. In the following figures, stress-strain graphs can be shown.

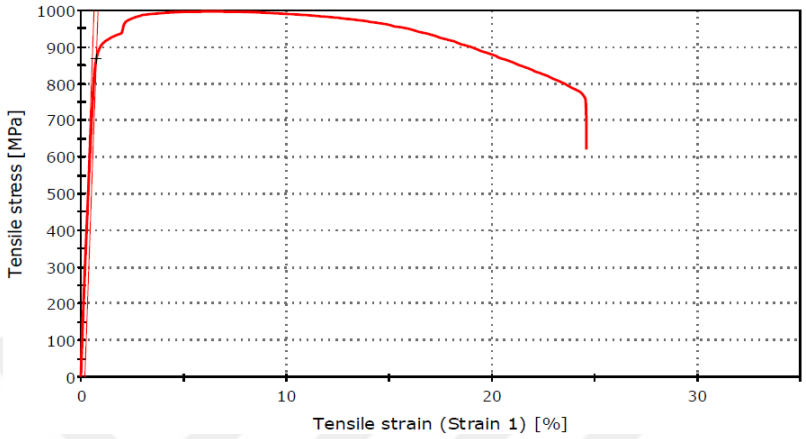

Figure 59: Stress vs. Strain Graph of X Direction [43]

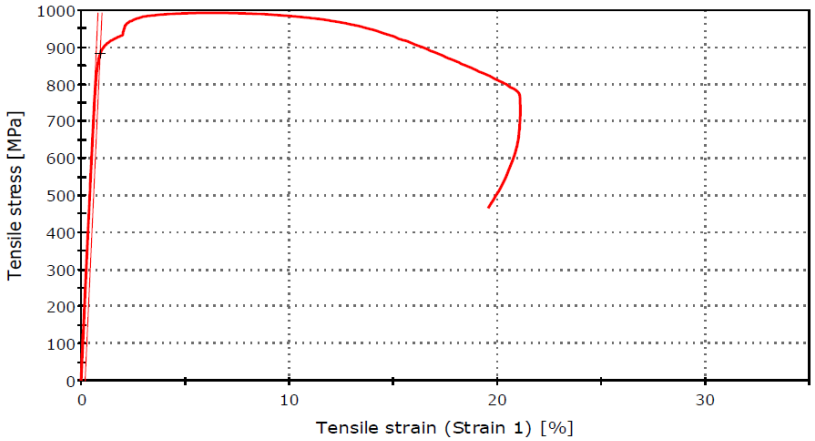

Figure 60: Stress vs. Strain Graph of Y Direction [43]

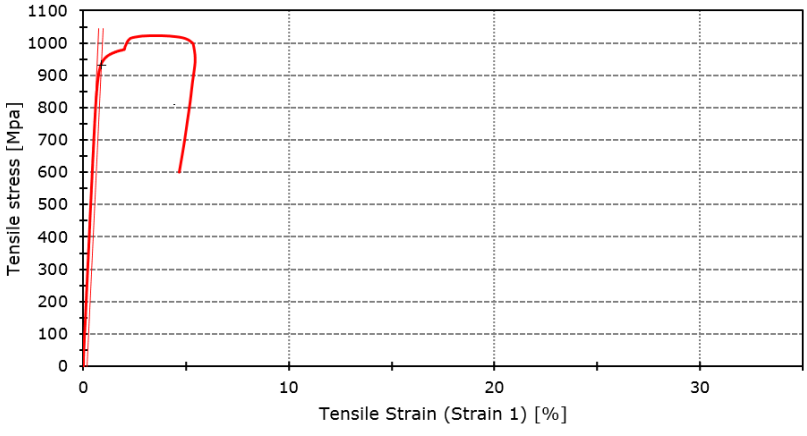

Figure 61: Stress vs. Strain Graph of Z Direction [43]

According to these graphs, there is a considerable difference in the Z direction even X and Y directions are almost the same. Since the results obtained in the Z direction have lower values one can be said that the parts which are produced perpendicular to the printing direction are weaker than the parts produced parallel to the printing direction.

As mentioned before, according to aviation regulations it is common and required to use minimum strength value considering the material is isotropic. This method provides conservative and trustable results. In Chapter 3, all the analyses were done by using this rule, and the final part was successfully tested. In the following analyses, optimizations are done on a cubic sample that has dimension of 40 mm. The anisotropic material properties of Ti64 are taken from the study of Yiğitbaşı S. which were shown in Table 1 before [43].

During the topology optimizations, all the cases are exposed to same boundary conditions and optimization settings. The material is selected as Ti64, and mass of the first volume is obtained as 0.277 kg. One side of the cubic part is fixed, and the opposite side is selected as the force face in x and y directions. To be able to perform noticeable analyses the value of the force is determined as 4000N as shown in Figure 62. The response type is selected as 'Mass' and it is constrained as %10 to retain.

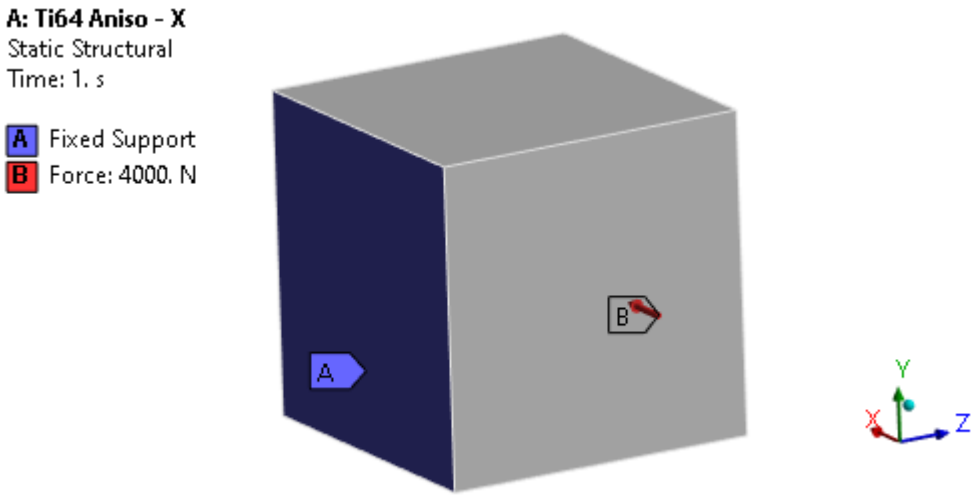

Figure 62: Boundary Conditions of the Anisotropic Analyses

The force is applied in both x and y directions as explained before. The validation analyses after the optimizations are shown in the following figures. Firstly, the analyses are carried out using isotropic material properties as made in previous chapters. After that, optimizations have been done considering anisotropic properties.

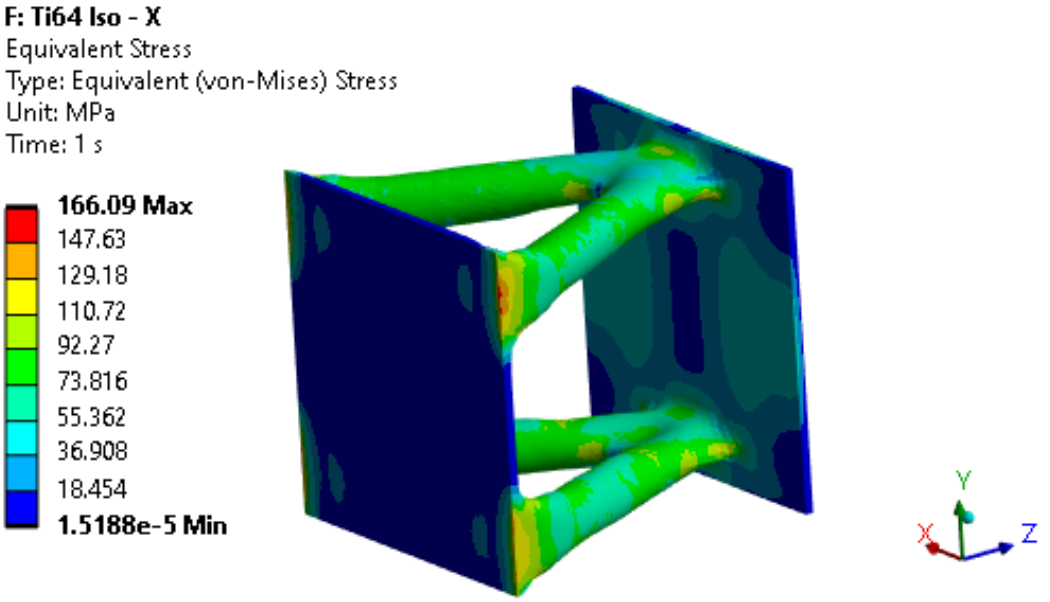

Figure 63: Maximum Von-Mises Stress of Optimized Volume in X Direction - Isotropic

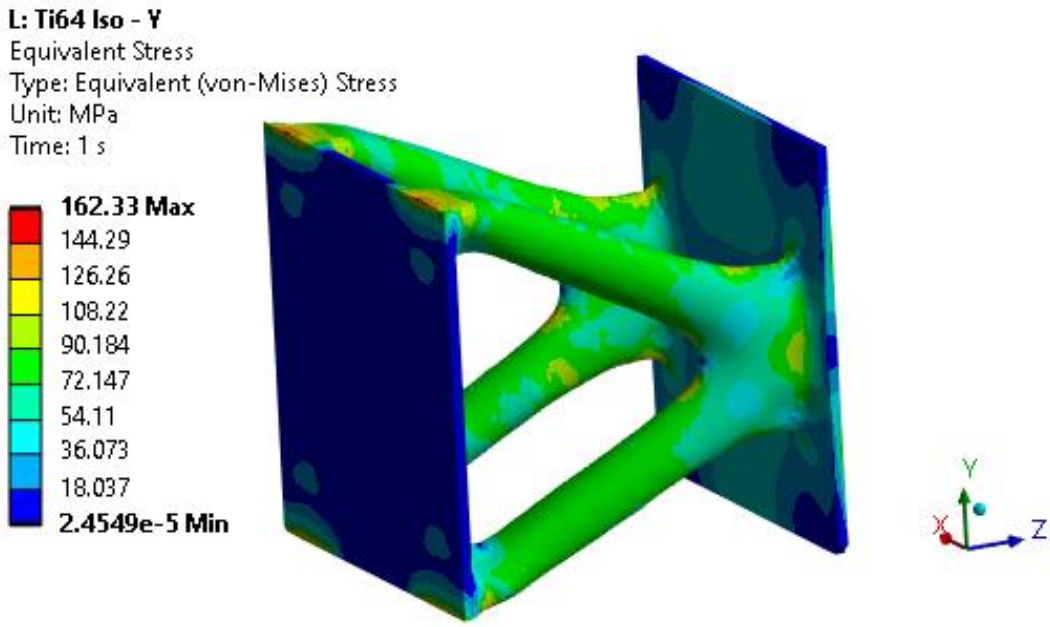

Figure 64: Maximum Von-Mises Stress of Optimized Volume in Y Direction - Isotropic

As shown in the figures, the optimizations are carried out almost the same for x and y directions. There is a small difference between the maximum von-mises stresses, and this difference may occur because of the sensitivity of the analyses and the program errors. The masses of the final volumes are obtained as 0.041 kg for both directions.

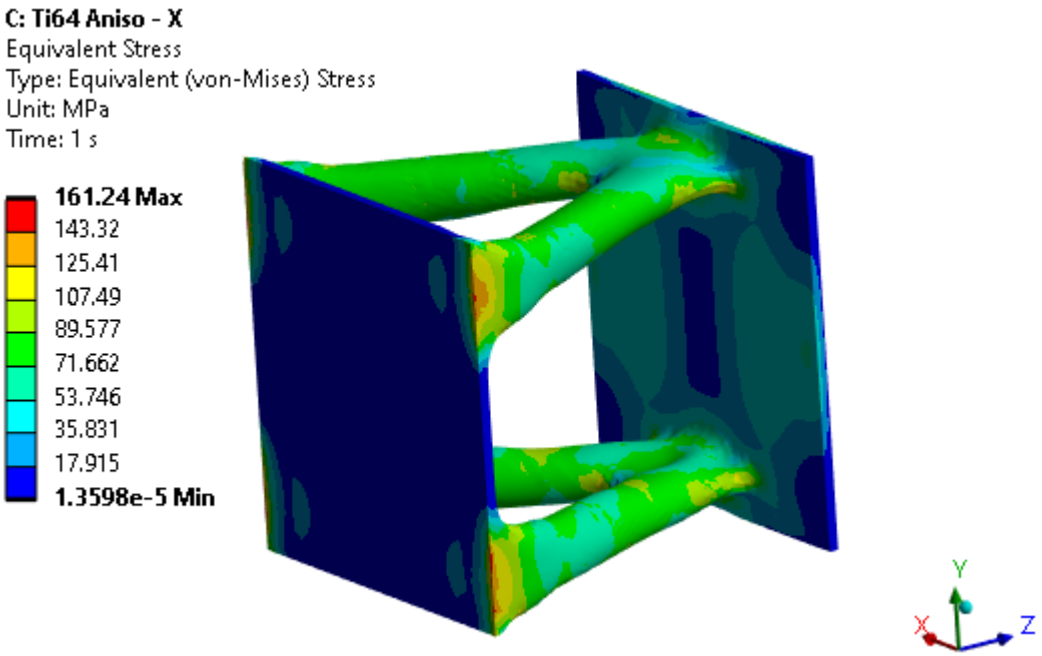

Figure 65: Maximum Von-Mises Stress of Optimized Volume in X Direction - Anisotropic

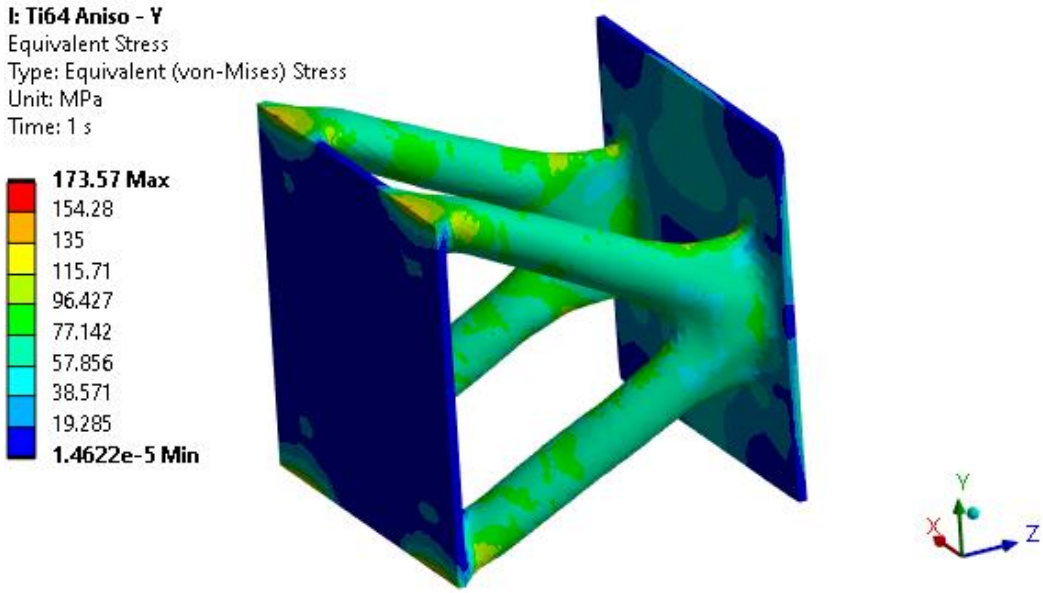

Figure 66: Maximum Von-Mises Stress of Optimized Volume in Y Direction - Anisotropic

The stress difference between the x and y directions increased for anisotropic analyzes as shown. Moreover, while there is a significant decrease in the x direction, the stress level increases dramatically in the y direction. Although the final masses are obtained as 0.041 kg as in previous analyses, the results show that anisotropic analysis has differences from the isotropic analyses.

In addition to the variable values in the stress levels, it is determined that there are also differences in the solution times of the analyses. Table 12 shows the solution times of the analyses.

Table 12: Solutions Times

Case	Time
Isotropic – X	07:41
Isotropic – Y	07:36
Anisotropic – X	06:29
Anisotropic – Y	09:49

There is a very small difference between isotropic analyses, as in stress analyses, but it has been observed that anisotropy also affects the solution times. Since the optimization constraint is selected as mass reduction, the final masses of the volumes were obtained the same.

Even if it is preferred to perform the optimization isotropic, the results showed that there are many different points during the solution, considering the anisotropy. For the Ti64, the anisotropy occurred due to the printing direction and nature of the additive manufacturing. Similar properties are expected for other AM materials, and many studies have proven this as discussed earlier. Since the aim is to observe results with implementation anisotropy to the topology optimization, the same studies and analyses are made using a composite material after Ti64.

4.2 ANISOTROPIC ANALYSES WITH COMPOSITE MATERIAL

The composite materials are known by their anisotropic properties in x and y directions so, to be able to see the differences same analyses are made on a cubic sample which has the same properties as before studies. The force and the boundary conditions are also kept the same. The material is selected as Epoxy Carbon UD Prepreg and the material properties are given in the below table.

Table 13: Material Properties of Carbon UD Prepreg

Direction	X	Y	Z
Young's Modulus [GPa]	121	8.6	8.6
Shear Modulus [GPa]	4.7	3.1	4.7
Tensile Stress Limit [MPa]	2231	29	29

The force is applied in both x and y directions and validation analyses after the optimizations are shown in the following figures. Since there is no data for the

isotropic properties, the only comparison is done for different directions with anisotropic properties.

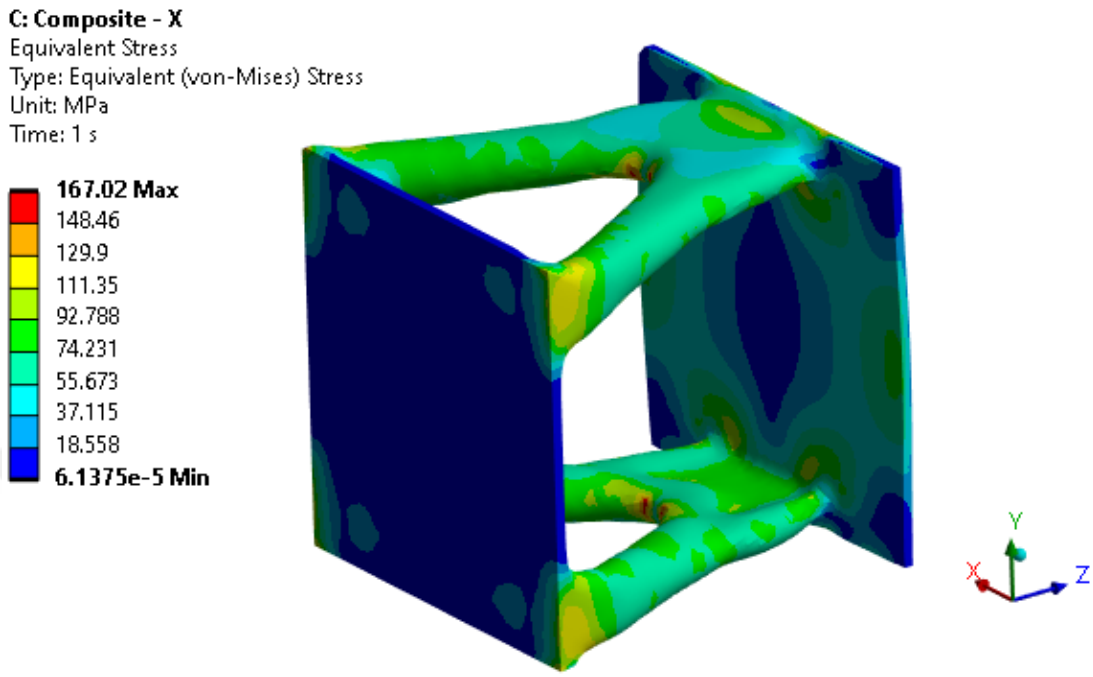

Figure 67: Maximum Von-Mises Stress of Optimized Volume in X Direction - Composite

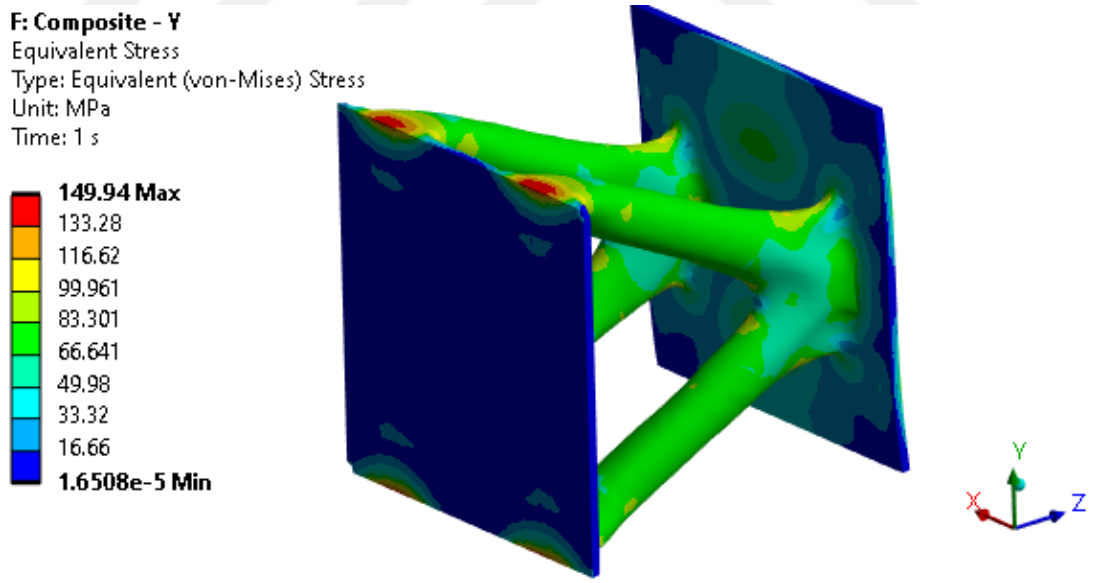

Figure 68: Maximum Von-Mises Stress of Optimized Volume in Y Direction - Composite

Although force and all optimization settings are kept the same, the maximum stresses on the optimized volume have different values, and, the masses of the result parts are 14.3 g for both directions. In addition, as in the previous studies, there is a noticeable difference in solution times. Table 14 shows these time values below.

Table 14: Solutions Times for Composite

Case	Time
Anisotropic – X	05:39
Anisotropic – Y	15:45

As shown in the table, there is a big difference in the solution times when compared with the times with Ti64. Also, even using the same methods and settings, the maximum stress levels occur very differently from each other.

Another remarkable point in the results obtained is that in the x-direction stress analysis, unlike the other analyses, the stress concentration occurred in the inner region of the part as shown in Figure 69. The difference here shows that the analyses made with anisotropic material properties also affect the volumes to be subtracted in the structure.

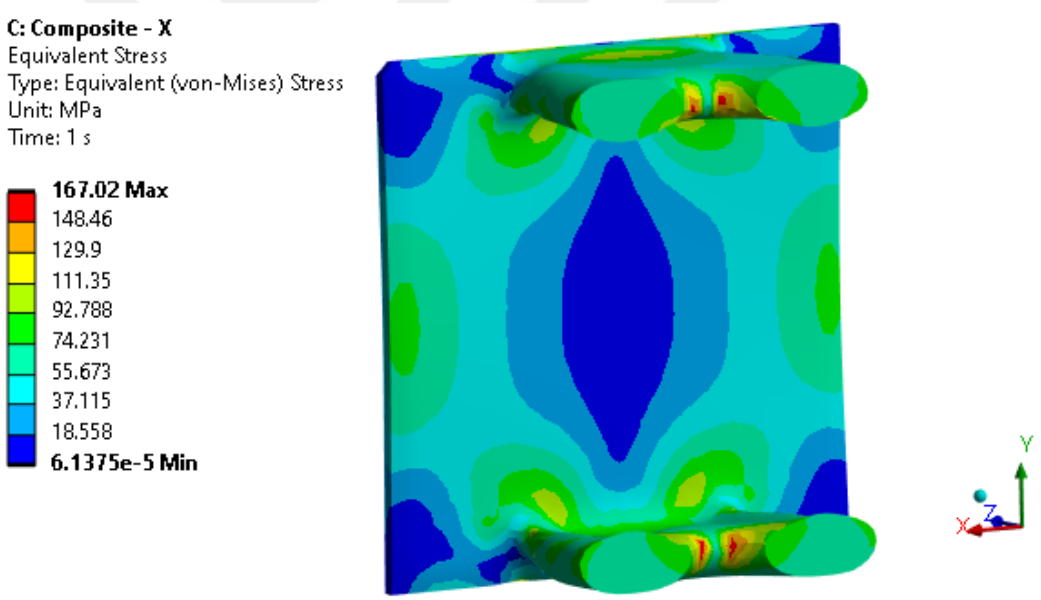

Figure 69: Sectioned View of Optimized Volume in X Direction - Composite

CHAPTER V
RESULTS AND DISCUSSION

With this study, implementation of the additive manufacturing constraints to topology optimization, and optimization analyses of an aircraft structural part are done. Since the planning of each production process was made in advance, the production of the optimized part could not be realized during the thesis study. However, the part was studied by considering all aviation standards, and the analyzes were carried out in this direction so, in future studies the part may be manufactured with the proper method mentioned earlier, and all the validation tests can be made on the produced part.

Firstly, the validation analyses for the current part are made to ensure that the given loads and the boundary conditions are valid. Then, different concepts are studied to get the most appropriate alternative. After that, topology optimization is applied to two different materials as aluminum and titanium. The goal is to achieve the best performance characteristics possible for a particular application.

The results from these analyses indicate that the aluminum component performs better than the titanium component under certain conditions, specifically when there are no points of stress concentration. It was observed that having a larger volume component with low-density characteristics, like aluminum, can lead to designs that are lighter in weight. This is contrasted with smaller-volume components made from high-density materials like titanium. The lower-density material, even though it occupies a larger volume, contributes less to the overall weight due to its inherent lightness. This principle is particularly valuable in applications where minimizing weight is a critical factor as in this study. So, the study confirms that using larger volumes of low-density materials can often result in more weight-efficient designs than using smaller volumes of high-density materials.

After the material selection is done, topology optimization is carried again out to obtain the final producible part by considering all the manufacturing constraints and the component requirements like bonding faces, fastener interfaces. As aluminum has

proven that it is advantageous in mass, the material is selected as AlSi10Mg which is one of the most common aluminum powders in the industry.

As a result, it was shown that using additive manufacturing for an optimized part in aerospace industry brings many advantages, especially in mass reduction. Additionally, the optimization results showed that the cost of the manufacturing process would be significantly reduced. Compared to traditional manufacturing methods, the amount of waste can be minimized by using less raw materials in the additive manufacturing process. In addition, the optimization process has also reduced the energy and time used in part production. This allows to reduce costs and increase efficiency.

In addition to the studies explained above, the effects of anisotropy on topology optimization were also studied by making case studies. The analysis results showed that anisotropy can have a significant effect on topology optimization, even if isotropic properties are generally preferred. In particular, the inclusion of anisotropy in analyzes has the potential to create lighter and more stiff structures for applications where loads are in a certain direction. Anisotropic optimizations can result in structures performing better under a given load, potentially leading to a more efficient use of energy and an overall more efficient design. Also, considering the anisotropy, the computation time and complexity of topology optimization have increased.

In future works, it is important to consider the anisotropy effect for the studies. Even the software and the methods are used mostly in isotropic properties, with the development of technology and the increase in computational capabilities, structural optimization analyses to be made by considering all the properties of materials can provide more efficient results than the current analyses.

REFERENCES

[1] RAO Singiresu S. (2009), *Engineering Optimization: Theory and Practice*, John Wiley & Sons Inc. Press, pp. 5.

[2] ZHU Jihong, ZHOU Han, WANG Chuang, ZHOU Lu, YUAN Shangqin and ZHANG Weihong (2020), "A Review Of Topology Optimization For Additive Manufacturing: Status And Challenges", *Chinese Journal of Aeronautics*, Vol. 34, No. 1, pp. 91-110.

[3] ABBEY Tony (2018), *Topology Optimization (Part 1)*, https://www.fetraining.net/topology-optimization-part-1/, DoA. 04.04.2023.

[4] TOP Neslihan, GÖKÇE Harun and ŞAHİN İsmail (2019), "Eklemeli İmalat için Topoloji Optimizasyonu: El Freni Mekanizması Uygulaması", *Journal of Selcuk-Technic*, Vol. 18, pp. 1-13.

[5] ZHU Ji-Hong, ZHANG Wei-Hong and XIA Liang (2016), "Topology Optimization in Aircraft and Aerospace Structures Design", *Arch Computat Methods Eng*, Vol. 23, pp. 595-622.

[6] SIGMUND Ole and MAUTE Kurt (2013), "Topology Optimization Approaches A Comparative Review", *Structural and Multidisciplinary Optimization*, Vol. 48, pp. 1031-1055.

[7] JANKOVICS Davin (2019), *Customized Topology Optimization for Additive Manufacturing* (Master's Thesis), Ontario Tech University, Oshawa.

[8] PERSSON Per-Olof (2004), *Structural Design Optimization*, http://persson.berkeley.edu/thesis/structoptim/, DoA. 10.04.2023.

[9] CHRISTENSEN Peter W. and KLARBRING Anders (2009), *An Introduction to Structural Optimization*, Springer Dordrecht, Linköping Sweden, pp. 5-6.

[10] LIU Shutian, LI Quhao, LIU Junhuan, CHEN Wenjiong and ZHANG Yongcun (2018), "A Realization Method for Transforming a Topology Optimization Design into Additive Manufacturing Structures", *Engineering*, Vol. 4, No. 2, pp. 277-285.

[11] SIGMUND Ole and BENDSØE Martin P. (2002), *Topology Optimization: Theory, Methods and Applications*, Springer Berlin, Heidelberg, pp. 2.

[12] GEBISA Aboma and LEMU Hirpa (2017), “A Case Study on Topology Optimized Design for Additive Manufacturing”, *IOP Conference Series: Materials Science and Engineering,* Vol. 276, pp. 12026, Stavanger, Norway.

[13] MICHELL AGM (1904), “The Limits of Economy of Material in Frame Structures”, *The London, Edinburgh, and Dublin Philosophical Magazine and Journal of Science,* Vol. 8, No. 47, pp. 589-597.

[14] JACOT Benjamin P. and MUELLER Caitlin T. (2017), “A Strain Tensor Method for Three-Dimensional Michell Structures”, *Struct Multidisc Optim*, Vol. 55, pp. 1819–1829.

[15] BENDSØE Martin P. and KIKUCHI Noboru (1988), “Generating Optimal Topologies In Structural Design Using A Homogenization Method”, *Computer Methods in Applied Mechanics and Engineering*, Vol. 71, No. 2, pp. 197-224.

[16] GUNWANT Dheeraj and MISRA Anadi (2012), “Topology Optimization of Continuum Structures Using Optimality Criterion Approach in Ansys”, *International Journal of Advances in Engineering & Technology*, Vol. 5, No. 1, pp. 470-485.

[17] THOMSEN Jan L. S. (1992), “Topology Optimization of Structures Composed of One or Two Materials”, *Structural Optimization*, Vol. 5, pp. 108-115.

[18] GROEN Jeroen and SIGMUND Ole (2017), “Homogenization-Based Topology Optimization for High-Resolution Manufacturable Micro-Structures”, *International Journal for Numerical Methods in Engineering*, Vol. 113, No. 8, pp. 1148-1163.

[19] BENDSØE Martin P. (1989), “Optimal Shape Design As A Material Distribution Problem”, *Structural Optimization 1*, Vol. 1, pp. 193-202.

[20] ZHOU Ming and ROZVANY George I. N. (1991), “The COC Algorithm, Part II: Topological, Geometrical and Generalized Shape Optimization”, *Comput. Methods Appl. Mech. Eng.*, Vol. 89, No. 1-3, pp. 309-336.

[21] XIE Yi-Min and STEVEN Grant P. (1993), “A Simple Evolutionary Procedure for Structural Optimization”, *Computers & Structures*, Vol. 49, pp. 885-896.

[22] XIE Yi-Min and HUANG Xiaodong (2010), “A Further Review of ESO Type Methods for Topology Optimization”, *Structural and Multidisciplinary Optimization,* Vol. 41, pp. 671-683.

[23] MARCK Gilles, NEMER Maroun, HARION Jean-Luc, RUSSEIL Serge and BOUGEARD Daniel (2012), "Topology Optimization Using the SIMP Method for Multiobjective Conductive Problems", *Numerical Heat Transfer Part B-fundamentals*, Vol. 61, No. 6, pp. 439–470.

[24] YANG Xiao-Qing, XIE Yuehong, STEVEN Grant P. and QUERIN Osvaldo M. (1998), "Bi-Directional Evolutionary Method for Stiffness Optimisation", *7th AIAA/USAF/NASA/ISSMO Symposium on Multidisciplinary Analysis and Optimization*, pp. 1483, St. Louis.

[25] QUERIN Osvaldo M., STEVEN Grant P. and XIE Yuehong (1998), "Evolutionary Structural Optimisation (ESO) Using a Bidirectional Algorithm", *Engineering Computations*, Vol. 15, No. 8, pp. 1031-1048.

[26] OSHER Stanley and SETHIAN James A (1998), "Fronts Propagating with Curvature-Dependent Speed: Algorithms Based on Hamilton-Jacobi Formulations", *Journal of Computational Physics*, Vol. 79, No. 1, pp. 12-49.

[27] HABER Robert B. and BENDSØE, Martin P. (1998), "Problem Formulation, Solution Procedures and Geometric Modeling - Key Issues in Variable-Topology Optimization", *7th AIAA/USAF/NASA/ISSMO Symposium on Multidisciplinary Analysis and Optimization*, pp. 1864, St. Louis.

[28] VAN DIJK N.M., MAUTE Kurt, LANGELAAR Matthijs and VAN KEULEN F. (2013), "Level-Set Methods for Structural Topology Optimization: A Review", *Structural and Multidisciplinary Optimization*, Vol. 48, No. 3, pp. 437-472.

[29] WASTI Sanjita and ADHIKARI Sushil (2020), "Use of Biomaterials for 3D Printing by Fused Deposition Modeling Technique: A Review", *Frontiers in Chemistry*, Vol. 8, pp. 315.

[30] HAINES Justin (2022), *History of 3D Printing: When Was 3D Printing Invented?*, https://all3dp.com/2/history-of-3d-printing-when-was-3d-printing-invented, DoA. 16.04.2023.

[31] 3D SYSTEMS (2021), *Our Story*, https://www.3dsystems.com/our-story, DoA. 16.04.2023.

[32] AÇIKGÖZ Cansu (2023), *Tarihçe*, https://yunus.hacettepe.edu.tr/cansu.acikgoz/webfinal/tarihce.html, DoA. 24.03.2023.

[33] DAVIES Sam (2020), *Exclusive Interview: Retiring Stratasys Founder Scott Crump on His 3D Printing Legacy*, https://www.tctmagazin e.com/additive-manufacturing-3d-printing-news/exclusive-stratasys-scott-crump-3d-printing-legacy, DoA. 16.04.2023.

[34] NGO Tuan, KASHANI Alireza, IMBALZANO Gabriele, NGUYEN Kate and HUI David S.C. (2018), "Additive Manufacturing (3D Printing): A Review of Materials, Methods, Applications and Challenges", *Composites Part B-engineering*, Vol. 143, pp. 172-196.

[35] KIRAN A. Sandeep Kranthi, VELURU Jagadeesh Babu, MERUM Sireesha, RADHAMANI A., DOBLE Mukesh, KUMAR T. S. Sampath and RAMAKRISHNA Seeram (2018), "Additive Manufacturing Technologies: An Overview of Challenges and Perspective of Using Electrospraying", *Nanocomposites*, Vol. 4, No. 4, pp. 190-214.

[36] LANCASTER Robert T., DAVIES Gareth, ILLSLEY Henry, JEFFS Spencer and BAXTER Gavin (2016), "Structural Integrity of an Electron Beam Melted Titanium Alloy", *Materials*, Vol. 9, No. 6, pp. 470.

[37] GE Aerospace (2021), *GE Aviation Reaches New Milestones In Advanced Manufacturing For More Fuel-Efficient Jet Engines*, https://www. geaerospace.com/press-release/other-news-information/ge-aviation-reaches-new-milestones-advanced-manufacturing-more, DoA. 21.04.2023.

[38] XIONG Yulin, YAO Song, ZHAO Zilong and XIE Yi (2020), "A New Approach to Eliminating Enclosed Voids in Topology Optimization for Additive Manufacturing", *Additive Manufacturing*, Vol. 32, pp. 101006, DOI: 10.1016/j.addma.2019.101006.

[39] MEISEL Nicholas A. and WILLIAMS Christopher (2015), "An Investigation of Key Design for Additive Manufacturing Constraints in Multimaterial Three-Dimensional Printing", *Journal of Mechanical Design*, Vol. 137, No. 11, pp. 100904/1-9, DOI: 10.1115/1.4030991.

[40] ZHAO Zi-long, ZHOU Shiwei, CAI Kun and XIE Yi (2020), "A Direct Approach to Controlling the Topology in Structural Optimization", *Computers & Structures*, Vol. 227, pp. 106141, DOI: 10.1016/j.compstruc.2019. 106141.

[41] LALEHPOUR Amirali and BARARI Ahmad (2016), "Post processing for Fused Deposition Modeling Parts with Acetone Vapor Bath", *IFAC-PapersOnLine*, Vol. 49, No. 31, pp. 42-48.

[42] ZOHDI Nima and YANG Chunhui (2021), "Material Anisotropy in Additively Manufactured Polymers and Polymer Composites: A Review", *Polymers*, Vol. 13, No. 19, pp. 3368.

[43] YİĞİTBAŞI T. Selen (2018), *Mechanical Properties Of Ti6Al4V Parts Produced By Electron Beam Melting And Topology Optimization In Different Building Directions* (Master's Thesis), Middle East Technical University, Ankara.

[44] TANG Ming and PISTORIUS Petrus Christiaan (2017), "Anisotropic Mechanical Behavior of AlSi10Mg Parts Produced by Selective Laser Melting", *JOM*, Vol. 69, No. 3, pp. 516-522.

[45] CARROLL Beth, PALMER Todd and BEESE Allison M. (2015), "Anisotropic Tensile Behavior of Ti–6Al–4V Components Fabricated with Directed Energy Deposition Additive Manufacturing", *Acta Materialia*, Vol. 87, pp. 309-320.

[46] SIMONELLI Marco, TSE Y. Y. and TUCK Christopher (2014), "Effect of The Build Orientation on The Mechanical Properties and Fracture Modes of SLM Ti–6Al–4V", *Materials Science and Engineering: A*, Vol. 616, pp. 1-11.

[47] YADOLLAHI Aref, SHAMSAEI Nima, THOMPSON Scott M., ELWANY Alaa and BIAN Linkan (2017), "Effects of Building Orientation and Heat Treatment on Fatigue Behavior of Selective Laser Melted 17-4 PH Stainless Steel", *International Journal of Fatigue*, Vol. 94, pp. 218-235.

[48] YANG Kaike, ZHU Jihong, WANG Chuang, JIA Dongsheng, SONG Longlong and ZHANG Weihong (2018), "Experimental Validation Of 3D Printed Material Behaviors and Their Influence on The Structural Topology Design", *Computational Mechanics*, Vol. 61, No. 5, pp. 581-598.

[49] BATTELLE MEMORIAL INSTITUTE (2022), Metallic Materials Properties Development and Standardization (MMPDS) Handbook - 17th Edition, 2022.

[50] DRAPER Susan L., LERCH Brad, ROGERS Richard, MARTIN Richard M., LOCCI I. E. and GARG Anita (2016), "Materials Characterization of Electron Beam Melted Ti-6Al-4V", *13th World Conference on Titanium*, pp.1433-1440, California.

[51] SHUNMUGAVEL Manikandakumar, POLISHETTY Ashwin and LITTLEFAIR Guy (2015), "Microstructure and Mechanical Properties of Wrought and Additive Manufactured Ti-6Al-4V Cylindrical Bars", *Procedia Technology*, Vol. 20, pp. 231-236.

[52] EOS (2015), *EOS 3D Printing Metal Powder - Titanium for 3D Printing*, https://www.eos.info/en/3d-printing-materials/metals/titanium-ti64-ticp, DoA. 29.04.2023.

[53] KEMPEN K., THIJS L., VAN HUMBEECK Jan and KRUTH Jean-Pierre (2012), "Mechanical Properties of AlSi10Mg Produced by Selective Laser Melting", *Physics Procedia*, Vol. 39, pp. 439-446.

[54] EOS (2015), *EOS 3D Printing Metal Powder - Aluminum for 3D Printing*, https://www.eos.info/en/3d-printing-materials/metals/aluminum-al, DoA. 29.04.2023.